Contribution of individual zinc fingers of WT1 in RNA aptamer binding

by

Julie Lynne Foster

M.Sc., University of Victoria, 2006

A Thesis Submitted in Partial Fulfillment of the
Requirements for the Degree of

MASTERS OF SCIENCE

in the Department of Biochemistry and Microbiology

Contribution of individual zinc fingers of WT1 in RNA aptamer binding

by

Julie Lynne Foster
B. Sc., University of Victoria, 2006

Supervisory Committee

Dr. Paul.J. Romaniuk, (Department of Biochemistry)
Supervisor

Dr. Claire. Cupples, (Department of Biochemistry
Departmental Member

Dr. Réal Roy, (Department of Biology)
Outside Member

Supervisory Committee

Dr. Paul.J. Romaniuk, (Department of Biochemistry)
Supervisor

Dr. Claire. Cupples, (Department of Biochemistry
Departmental Member

Dr. Réal Roy, (Department of Biology)
Outside Member

ABSTRACT

The WT1 gene encodes for a transcription factor which is mutated in approximately 15% of sporadic Wilms' tumors (Orkin *et al.*, 1984; Fearon *et al.*, 1990). Mutations in *WT1* are also associated with a number of clinical disorders such as Denys-Drash and Frasier syndromes, which are distinguished by genitourinary malformation and kidney disease (McTaggart *et al.,* 2001).

The nucleic acid binding domain of WT1 is comprised of four tandemly arranged C2H2 type zinc fingers (Haber *et al.*, 1990; Rauscher *et al.*, 1990; Morris *et al.*, 1991). The WT1 transcript is regulated by two different alternative splicing events. The first alternative splice introduces 17 amino acids between the proline-rich amino terminus and the zinc finger domain (Haber *et al.*, 1991). The second alternative splice inserts the amino acids KTS between zinc fingers 3 and 4 (Haber *et al.*, 1991). The +KTS and –KTS isoforms of WT1 have different nucleic acid binding specificities. The –KTS isoform readily binds to specific sequences in both DNA and RNA, while the +KTS isoform only binds to specific sequences in RNA (Zhai *et al.,* 2001). The RNA binding capabilities of the +KTS variant combined with its presence in spliceosomes

(Davies *et al*., 1998) and nuclear poly(A)+ ribonucleoprotein (Ladomery *et al.,* 1999), suggests that it is involved in RNA metabolism.

WT1 has been shown to interact with RNA through the zinc finger domain (Caricasole *et al*, 1996), but as of yet, there is not a purified crystal structure of WT1 interacting with RNA. There have been many experiments that have attempted to decipher the mechanism for WT1 RNA binding (Caricasole *et al*, 1996; Bardeesy and Pelletier, 1998). One zinc finger knock-out experiment has proposed that it is zinc finger number 1 which plays the most important role in this RNA interaction (Caricasole *et al*, 1996) while another suggests that it is finger 4 (Bardeesy and Pelletier, 1998).

In order to determine which zinc finger of WT1 is the most crucial for RNA binding, WT1 swap mutants and deletion mutants were created by PCR and a filter binding assay was employed to determine dissociation binding constants of the mutant proteins with the WT1-specific RNA aptamer Pel22. The mutant W12P8W4, which has finger 3 of WT1 replaced with finger 8 of the zinc finger protein p43, demonstrated a relative affinity for Pel22 of less than 0.29. The deletion mutant WT1ΔF4 which had finger 4 of WT1 deleted showed no affinity for Pel22 RNA, while the mutant Wp4 which had finger 4 of WT1 replaced with finger 9 of p43 demonstrated a 10 times greater affinity for Pel22 than wild type WT1. These results suggest that finger 3 makes important residue-base contacts with the RNA and that perhaps finger 4 confers some sort of stability to the WT1-RNA complex.

Table of Contents

List of Tables

List of Figures

List of Abbreviations

Bp: base pair

BSA: bovine serum albumin

cDNA: complementary deoxyribonucleic acid

cpm: counts per minute

deoxynucleotide triphospates:

dATP, deoxyadenosine triphosphate

dCTP, deoxycytidine triphosphate

dGTP, deoxyguanine triphosphate

dTTP, deoxythymidine triphosphate

DNA: deoxyribonucleic acid

DTT: dithiothreitol

E. coli: *Escherichia coli*

EDTA: ethylenediamine-tetraacetic acid

IPTG: isopropyl-β-D-thiogalactopyranoside

LB: Luria-Benton broth

mRNA: messenger ribonucleic acid

MW: molecular weight

NMR: nuclear magnetic resonance

Nucleotide triphosphates:

ATP, adenosine triphosphate

CTP, cytidine triphosphate

GTP, guanine triphosphate

UTP, uridine triphosphate

PAGE: polyacrylamide gel electrophoresis

PMSF: phenylmethylsulfonyl fluoride

RNA: ribonucleic acid

rRNA: ribosomal ribonucleic acid

RNP: ribonucleoprotein

SDS: sodium dodecyl sulphate

TBE: Tris, borate, EDTA

TFIIIA: Transcription Factor III A

tRNA: transfer ribonucleic acid

Tris-HCL: tris-(hydroxymethyl)-aminomethane hydrochloride

WT1: Wilms' tumor suppressor protein

Acknowledgements

I would like to thank many people who have helped me along this journey. First I would like to thank Paul Romaniuk for his help and guidance through this process. A big shout out to Tristen Weiss for all of the good times and bad times that we shared together in the "wonderful" world of science. I really appreciate my family and Scott for putting up with me for the past two years, especially through the 'write-up' process. I would also like to thank past members of our lab, Megumi Takiguchi and Heather Croft for their help in the lab and good times at the start of my Masters.

Finally I want to thank all the other people in the department that I've had great conversations with – it made the past 2 years enjoyable and go by fast!

Chapter 1. Overview and Introduction

RNA is essential for cell viability and maintenance. It is involved in many key functions within the cell, such as DNA replication, transcriptional control and protein synthesis. Many of these processes involve the interaction of RNA with specific protein partners. For instance, RNA protein complexes form the ribosome and the spliceosome (Yang and Walsh, 2005), which are essential for protein synthesis. During translation, tRNA's are found bound to aminoacyl-tRNA synthetases, and RNPs (ribonucleoprotein particles) bind to RNA in post transcriptional regulation of gene expression (Jones *et al.*, 2001). It is clear that cellular biological functions depend upon the interaction of RNA and proteins; however, the specific mechanisms of these interactions are difficult to elucidate (Jones *et al.*, 2001; Brown, 2005).

At the heart of the problem lies the lack of RNA-protein structures that have been solved by crystallography and NMR. RNA-protein complexes are technically difficult to isolate, leading to problems in obtaining good structural resolution (Ke and Doudna, 2004). Other methods to study interactions between RNA and proteins have been developed. Insight into the mechanisms of the binding of RNAs to their specific protein partners from such studies will lead to further investigation into the role of these complexes in specific cellular processes.

In this study, the mechanism of RNA binding by the zinc finger protein Wilms' tumor suppressor protein (WT1) was investigated. This zinc finger protein has the ability to bind specifically to both DNA and RNA. The binding of WT1 to DNA is well understood and it was the goal of this project to achieve a similar level of understanding about WT1-RNA interactions.

1.1. Zinc Finger proteins and nucleic acid interactions

1.1.1. Zinc Fingers

The zinc finger motif has been extensively studied since the structure was first recognized in the transcription factor TFIIIA (Miller *et al.*, 1985). Originally, the zinc finger motif was identified as a 30 amino acid motif, containing conserved cysteine and histidine residues that co-ordinate to zinc; however, other zinc binding motifs have now been identified such as the treble clef finger and the zinc ribbon (Laity *et al.*, 2001; Krishna *et al.*, 2003).

Zinc finger domains are responsible for many cellular interactions, and can interact with nucleic acids (both RNA and DNA) and also with specific domains in other proteins (including zinc finger domains). Not surprisingly, proteins containing zinc fingers are involved in many cellular processes such as transcription, translation, metabolism, cell proliferation, and apoptosis (Krishna *et al.*, 2003). It is quite clear that structural studies of zinc finger proteins are extremely important. Structural evidence will provide essential clues as to the inherent function and biology of this wide spread class of molecules. This in turn will hopefully give us insights into disease mechanisms associated with specific zinc finger proteins.

1.1.2. C2H2 Zinc Finger Family

The C2H2 type of zinc finger motif was first discovered in the transcription factor IIIA isolated from the oocytes of *Xenopus laevis* (Miller *et al.*, 1985). The motif has since been found in many other transcription factors and is the most abundant DNA binding motif found within the human genome (Laity *et al.*, 2001;

Venter *et al.*, 2001). The classical C2H2 zinc finger consists of 28-30 amino acid residues, which compose a ββα fold. Each zinc finger contains two invariant cysteine residues and two invariant histidine residues which co-ordinate a single zinc ion (Figure 1). The zinc ion is tetrahedrally coordinated between the two cysteines at one end of the β-sheet and the two histidines at the C-terminal portion of the α helix (Corbi *et al.*, 2004).

As more zinc finger sequences were discovered, it became apparent that the C2H2 family of zinc fingers share the consensus sequence (F/Y)-X-C-X_{2-5}-C-X_3-(F/Y)-X_5-ψ-X_2-H-X_{3-5}-H, where X represents any amino acid and ψ is a hydrophobic residue. This zinc finger motif can occur in multiple copies to give rise to a zinc finger domain containing many zinc fingers. The most common linker sequence, which is found in approximately half of the known C2H2 zinc finger proteins, is TGEKP, or variants that very closely resemble this sequence. The linkers are well ordered and mutational analyses have shown that linker sequences are not just passive, but are possibly involved in stabilizing the α helix by capping the C-terminal end (Choo and Klug, 1993; Clemens *et al.*, 1993; Laity *et al.*, 2000).

Although most C2H2 type zinc finger proteins function as transcription factors, and are most widely known for their DNA binding capabilities, it has recently become apparent that some of these DNA binding proteins can also act as RNA binding proteins (Cassiday and Maher, 2002).

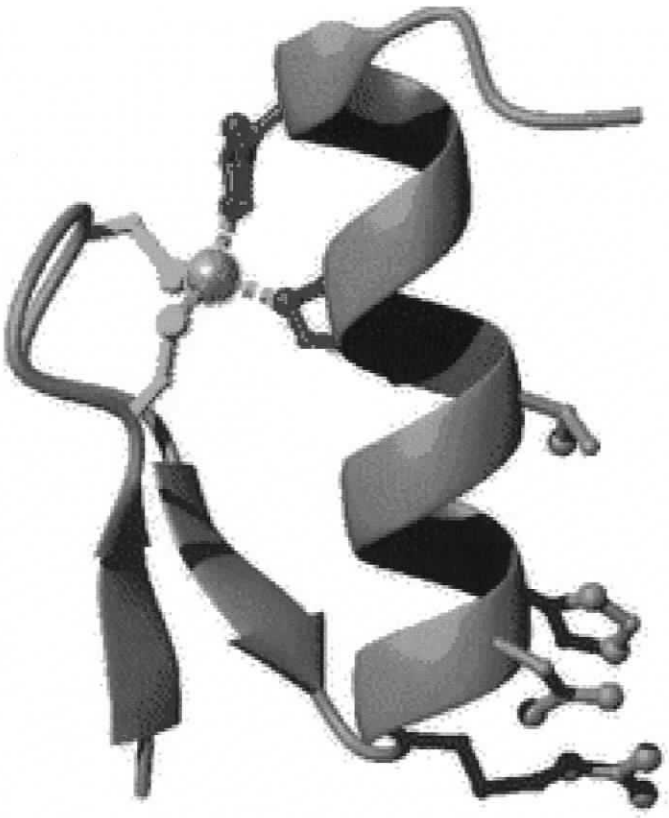

Figure 1. A ribbon diagram of finger 2 from Zif268 representing the C2H2 zinc finger motif (Pabo *et al.*, 2001). The zinc is co-ordinated by two cysteine side chains (yellow) and two histidine side chains (red).

The dual specificity of these proteins raises structural and mechanistic questions that are generally still unanswered. How can a single polypeptide chain bind to nucleic acids that are likely to be distinct in both secondary and tertiary structure? Is the mechanism different for RNA binding compared to DNA binding, or are these proteins interacting with regions of RNA that fold to mimic B-form DNA? Some of the breakthrough evidence that highlights the differences between RNA and DNA binding by the C2H2 type of zinc finger proteins is presented below.

1.1.3. DNA recognition by C2H2 type zinc finger proteins

Solution of the crystal structure of the zinc finger domain from Zif268 bound with DNA served as a model for the mode of DNA recognition by this class of molecules (Pavletich and Pabo, 1991). The DNA binding domain of Zif268 contains 3 zinc fingers (Figure 2). The three fingers of Zif268 are oriented so that finger 1 is at the 3' end of the sense DNA strand and finger 3 is at the 5' end. The α helical portion of each finger fits into the major groove of the DNA, and binding of successive fingers causes the protein to wrap around the DNA. It is within the α helix, often termed the recognition helix, where specific amino acid-base contacts occur. Each zinc finger occupies an overlapping sub site of 4 bp on the DNA, however most fingers make contacts with 3 consecutive base pairs within the sub site (mostly with the sense strand). By convention, amino acid residues are numbered relative to the start of the recognition helix, and the residues that make base contacts with DNA are at positions -1, 2, 3 and 6. Typically, the residue at position -1 contacts the 3' base of the sub site, residue at position 3 of helix contacts the central base and the

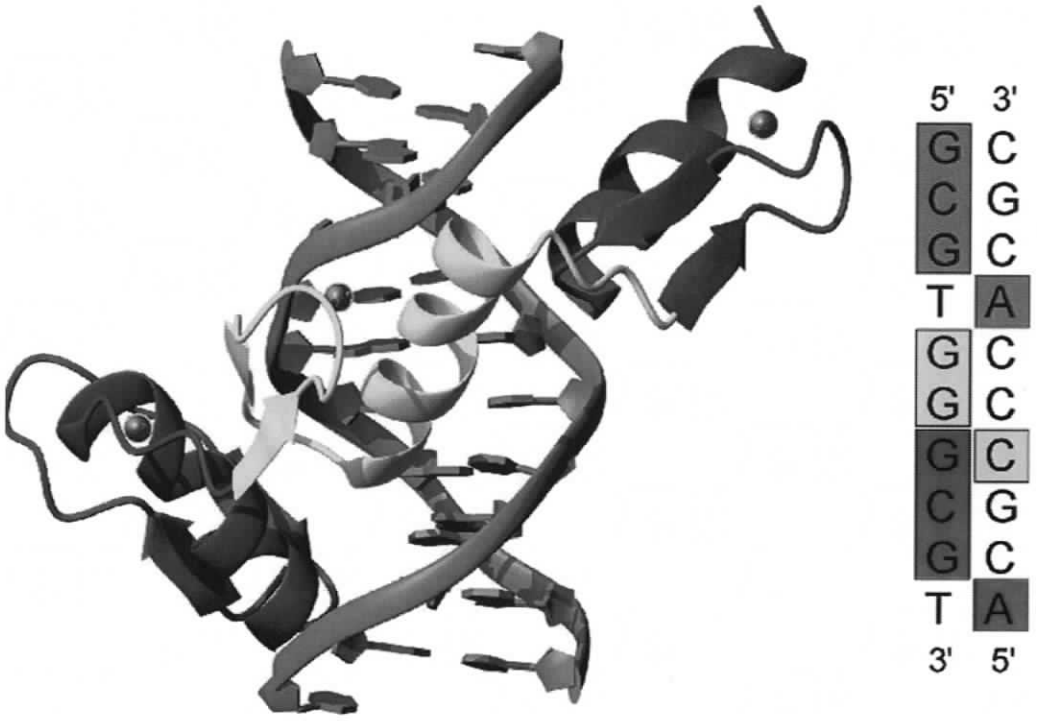

Figure 2. Left. The Zif268-DNA complex (Pabo *et al.*, 2001). A ribbon diagram showing each of the three zinc fingers of Zif268 bound in the major groove of the DNA. The three fingers are orientated so that finger 3 (purple) is positioned at the 5' end of the sense strand and finger 1 (red) is positioned at the 3' end of the sense strand. Right. Zif268 consensus sequence. Bases are colour coded by which zinc finger makes residue-bases contacts.

residue at position 6 tends to contact the 5' base. Normally The DNA conformation is similar to B-form DNA, but has a wider and deeper major groove (Pavletich and Pabo, 1991).

1.1.4. RNA recognition by C2H2 type zinc fingers

The first zinc finger protein found to interact with RNA was TFIIIA (Barrett *et al.*, 1983). In *Xenopus* oocytes TFIIIA acts as a transcription factor, regulating the transcription of the 5S RNA gene, and it is also involved in the storage of 5S RNA (Barrett *et al.*, 1983). It is well established that the secondary and tertiary structure of RNA is more complex than that of DNA. It is comprised of internal loops and helical elements closed by hairpin loops (Holbrook, 2005); thus, the finding that TFIIIA could bind to DNA and RNA raised the very interesting structural question of how the same protein could bind such structurally distinct molecules.

Some of the first insights into the mechanism of RNA binding by a zinc finger protein came from studies of TFIIIA from our laboratory. Binding experiments with TFIIIA and internal deletion and truncated 5S RNA mutants found that TFIIIA interacts with both arms of the 5S RNA molecule (Romaniuk *et al.*, 1987). It was also found that 5S RNA mutants containing substitutions of bases within loop A exhibited reduced TFIIIA binding affinity, indicating that loop A is essential for the interaction. (Romaniuk, 1989). The role of TFIIIA zinc fingers were studied and it was found that zinc fingers 4-6 are most crucial for TFIIIA affinity for 5S RNA (Clemens *et al.*, 1993). Further *in vitro* mutational analysis showed that finger 6 of TFIIIA makes a significant contribution to 5S binding (Hamilton *et al.*, 2001).

In 2003, the laboratory of Aaron Klug solved the crystal structure of TFIIIA zinc fingers 4-6 complexed with a truncated version of 5S RNA (Figure 3) (Lu *et al.*, 2003). Results from these studies revealed that RNA binding by TFIIIA occurs by a mechanism that was predicted by the earlier mutational studies. The zinc-fingers interact with the backbone of a double helix, and the zinc-fingers specifically recognize individual bases that are easily accessed in an otherwise complexly folded 'loop ' region of RNA (loop A) (Lu *et al.*, 2003). Specifically, zinc finger 5 uses side chains from the α helix to bind to the major groove backbone of a double helical region of the RNA. Both fingers 4 and 6 form specific contacts in loop regions of 5S RNA, which is mediated through the N-terminal ends of their α helices. Specifically, residues -2, -1, +1 and +2 of the α helix of finger four makes base and backbone contacts within the RNA, whereas residues positions -1, +1 and +2 of finger 6 make contacts within loop A of 5S RNA, which includes a stacking interactions between Trp177 and A11 (Lu et al., 2003).

The three dimensional structure of TFIIIA complexed with 5S RNA provides a good starting point for the study of other zinc finger RNA interactions; however, it is not absolute. Differences in RNA secondary and tertiary structure, specific amino acid residues at key positions, and the number of zinc fingers involved, all play a significant role in determining the RNA binding mechanism of a protein.

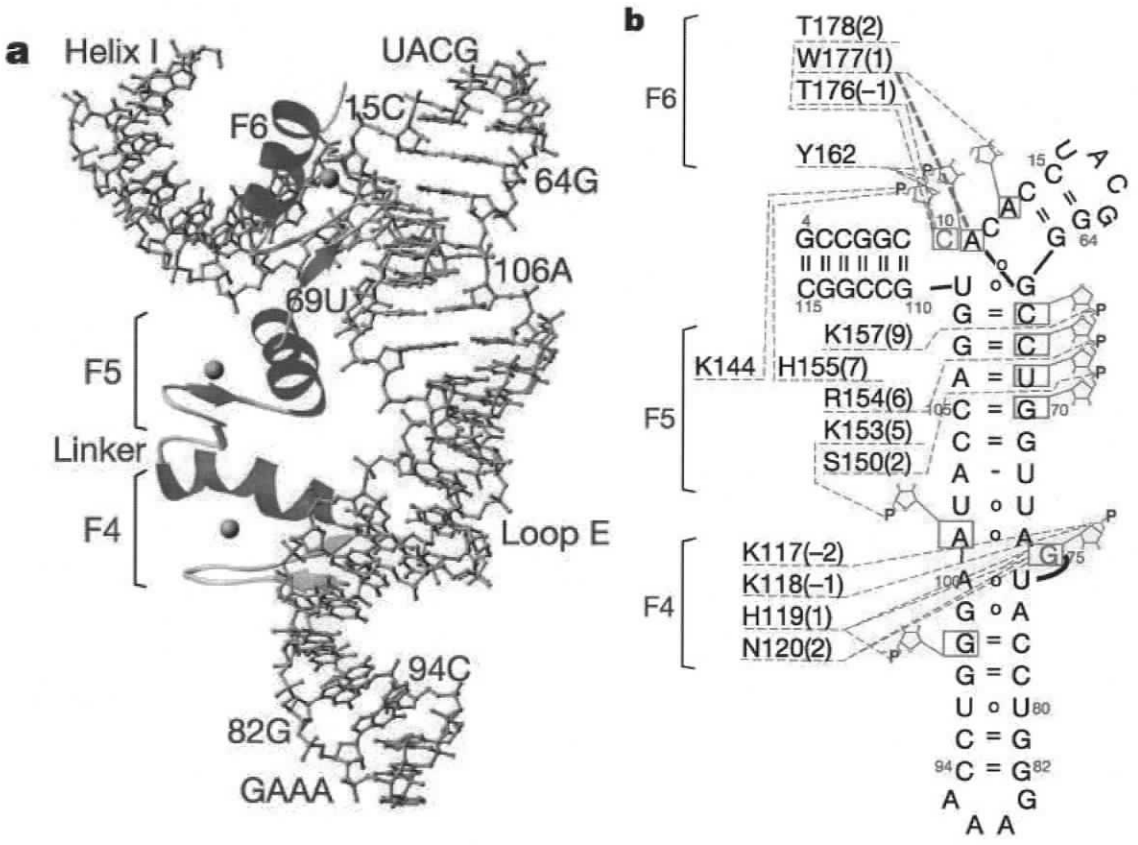

Figure 3. a) Overall view of the complex of TFIIIA zinc fingers 4-6 and truncated 5S RNA. The RNA is represented as a ball-and-stick model and zinc ions are represented by purple balls. b) Hydrogen-bond interactions between protein and RNA. Amino acid helical positions in brackets. Nucleotides involved in interactions are boxed, and bases shown in blue make direct interactions with protein. The broken green line indicates stacking of aromatic rings (Lu *et al.*, 2003).

1.2. WT1: The Zinc Finger Protein Under Investigation in This Study

1.2.1. Wilms' Tumor

In 1887 at the General Infirmary in Leeds England, the first successful surgery was performed by Dr. Thomas Jessop (1837-1903) which removed a large malignant growth from the left kidney of a 2-year old child (Willetts, 2003). It wasn't until 22 years later that the surgeon Max Wilms (1867-1918) described this type of malignancy in a monograph about "mixed tumors" (Metzger and Dome, 2005). The nephroblastoma has come to be known as Wilms' tumor. It represents ~8% of all pediatric tumors and is the most common cancer of the urinary tract in children (Matsunaga, 1982). It affects 1 in 10, 000 children under the age of 16; it is usually detected in children before the age 5.

The tumor itself is derived from pluripotent embryonic renal precursors and is tri-phasic. In other words, it is composed of three histological elements: epithelial, stromal and undifferentiated mesenchymal cells (Lee and Haber, 2001). Although all of the gene mutations associated with Wilms' tumors have not been identified, ~15% of sporadic Wilms' tumors have been associated with mutations and deletions that have been mapped to chromosome 11 band p13 (Orkin *et al.*, 1984; Fearon *et al.*, 1990). The gene present at this genetic locus was determined to be a tumor suppressor gene.

A predisposition to Wilms' tumor can often be linked to one of four developmental syndromes: Beckwith-Wiedemann, WAGR (Pendergrass, 1976; Riccardi *et al.*, 1978; Francke *et al.*, 1979), Denys-Drash (Pelletier *et al.*, 1991), and

Frasier (Barbaux *et al.*, 1997; Klamt *et al.*, 1998; Kohsaka *et al.*, 1999), with documentation of the *WT1* gene having mutations in the last three syndromes. The characteristics of all four syndromes are summarized in Table 1. Here we will focus mainly on Denys-Drash and Frasier Syndromes. These two syndromes are characterized by male pseudohermaphroditism (ambiguous external and internal genitalia), progressive glomerular disease, and the development of genitourinary tumors (Little and Wells, 1997; McTaggart *et al.*, 2001; Guo *et al.*, 2002).

The main phenotypic distinction between Frasier and Denys-Drash syndromes is differences in nephropathy. Denys-Drash patients generally show diffuse mesangial sclerosis compared with Frasier patients, who demonstrate focal and segmental glomerulosclerosis (Saylam and Simon, 2003).

1.2.2. Identification of the Wilms' Tumor gene

In 1990 Housman's group isolated and characterized the gene found at the human chromosome 11 Wilms' tumor locus (Call *et al.*, 1990). They characterized a transcript that spanned approximately 50 Kb within the region of human chromosome 11p13. The nucleotide sequence of the isolated transcript was determined, and the predicted amino acid sequence of the product was deduced. Of particular interest was the C-terminal region of the Wilms' tumor gene (specifically nucleotides 670 to 1002 of their isolated clones). It encoded four contiguous zinc finger motifs, suggesting that the Wilms' tumor gene product might recognize DNA. Furthermore, a proline/glutamine rich region was predicted in the Wilms' tumor polypeptide, and this motif combined with the zinc finger motifs, gave the first evidence that the protein encoded by the Wilms' tumor gene was a transcription factor. The gene present at the

Table 1. Human congenital syndromes associated with predisposition to Wilms' Tumor (WT) (taken from Discenza and Peletier, 2004).

Syndrome	Phenotype	Germ Line Abnormality
WAGR	WT, aniridia, genitourinary defects, mental retardation	Hemizygous deletion at chromosome 11p13
Beckwith-Wiedemann	Organomegaly, hypoglycemia, umbilical hernia, predisposition to adrenal cortex carcinoma, hepatoblastoma, WT	Precise genetic lesion unclear; loss of imprinting of several genes, including IGF-II, H19 and $p57^{kip2}$ has been reported; rare mutation found in $p57^{kip2}$
Denys-Drash	WT, genitourinary defects, diffuse mesangial sclerosis	Heterozygous mutations in WT1
Frasier	Genitourinary defects, focal segmental glomerular sclerosis, ambiguous genitalia, low risk of WT	Heterozygous point mutation at the donor splice site of intron 9 in WT1

Wilms' tumor locus was subsequently named *WT1*.

1.2.3. Structure of WT1

The *WT1* gene consists of 10 exons, and encodes for a protein of approximately 50 kDA. The WT1 gene product, Wilms' Tumor Suppressor Protein (WT1), is composed of two distinct functional domains: a C-terminal zinc finger domain consisting of four C2H2 type zinc fingers, and an N-terminal proline/glutamine rich transactivation domain (Figure 4) (Haber *et al.*, 1990; Rauscher *et al.*, 1990; Morris *et al.*, 1991). The last 3 zinc fingers of the C-terminal domain have a high sequence homology to the early growth response 1 and 2 gene products EGR1 and EGR2 respectively (Joseph *et al.*, 1988; Sukhatme *et al.*, 1988). Whereas all of the zinc fingers in EGR1 are encoded by a single exon, each zinc finger of WT1 is encoded by its own exon (Haber *et al.*, 1991). This difference indicates that while the gene products share high homology, they have a different genetic structure and therefore have not evolved from the same origin.

1.2.4. Alternative splicing of the WT1 gene product

There are four separate transcripts that are expressed by the *WT1* gene. These are derived from alternative splicing events (Figure 5). The first alternative splice site is found between the proline-rich amino terminus and the zinc finger domain. It inserts an entire exon encoding 17 amino acids (Haber *et al.*, 1991). The second alternative splice results in a 3 amino acid insertion (KTS) between zinc fingers 3 and 4. The +KTS insertion was the first alternative splice site discovered within a transcription factor that interrupts the highly conserved linker region between

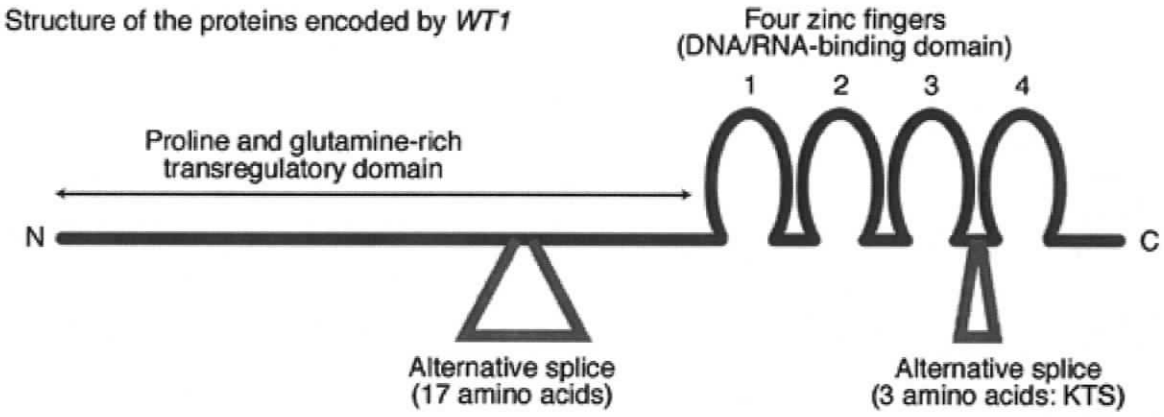

Figure 4. Structure of the proteins encoded by *WT1* (Brown and Malik, 2001). The two alternative splice sites are designated by purple triangles.

adjacent zinc fingers (Haber *et al.*, 1991). Furthermore, there have been three translation initiation sites identified in the WT1 mRNA (Bruening and Pelletier, 1996; Scharnhorst *et al.*, 1999) (Figure 6), and there have also been reports of an RNA editing event that replaces leucine 280 in the WT1 protein with a proline.When these modifications are combined with the four isoforms derived from alternative splicing events, it would be expected that there could be at least 24 different isoforms of WT1 produced (Discenza and Pelletier, 2004). RNase protection analysis performed by Haber *et al.* (1991) revealed that the most common isoform of the WT1 transcript is the variant that contains both alternative splices. In contrast, the least common transcript is that comprised of no splice insertions. Interestingly, of the two different splice variants, only the +KTS insertion is present in lower vertebrates (fish, amphibian and birds) indicating its importance in chordate development (Miles *et al.*, 2003). The +KTS to -KTS ratio is in the range of 1.1-1.5:1 and is conserved over all gnathostome classes (Kent *et al.*, 1995), and exemplifies the importance of isoform ratio in WT1 function and development. The biological importance of this ratio is most dramatically observed in Frasier syndrome where a reduced expression of WT1 +KTS transcripts results in severe developmental abnormalities (Barbaux *et al.*, 1997).

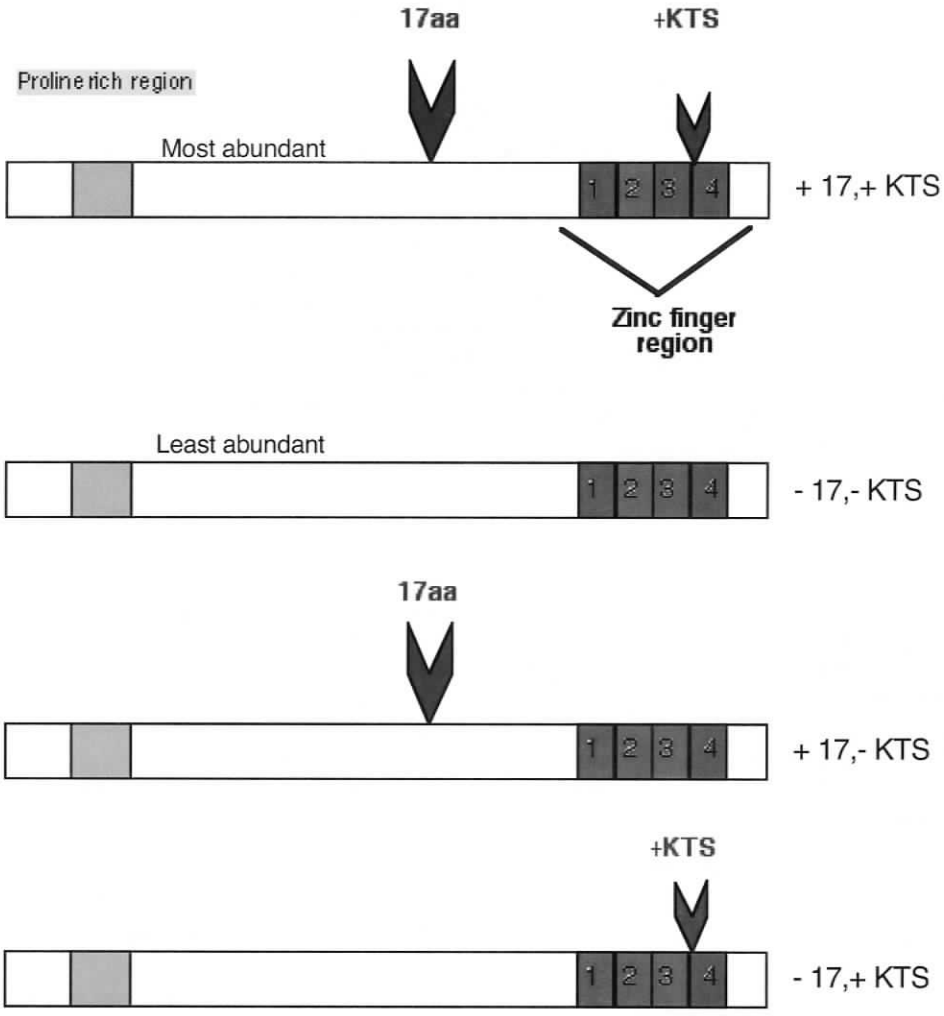

Figure 5. Schematic diagram representing the 4 most common isoforms of WT1 (Hirose, 1999).

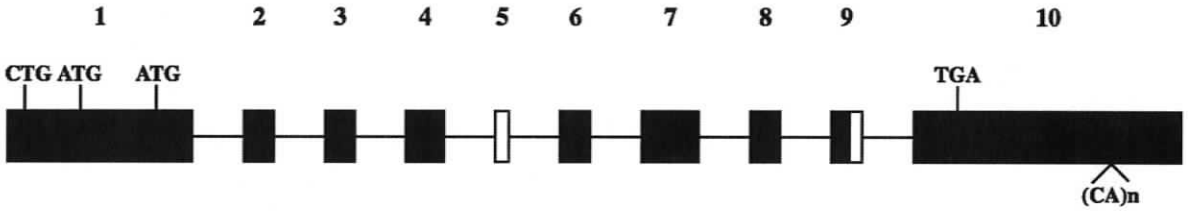

Figure 6. Schematic diagram the three alternative start sites within the WT1 gene. (Discenza and Peletier, 2004).

1.2.5. WT1 function

The presence of a C2H2 type zinc finger region in conjunction with a proline/glutamine-rich transregulatory domain indicates that WT1 can function as a transcription factor. Both of these domains are common to many transcription factors, and this function was confirmed by Haber *et al.* (1991). *In vivo* and *in vitro* studies also indicate that WT1 can act both as a transcriptional activator and a transcriptional repressor. Some of the WT1 target genes whose promoters have been repressed by WT1 in transient transfection assays are ERG1 (Madden *et al.*, 1991), PDGF-A (Gashler *et al.*, 1992; Wang *et al.*, 1992), insulin-like growth factor receptor (Werner *et al.*, 1993; Werner *et al.*, 1995), Bcl2 (Hewitt *et al.*, 1995), and even WT1 itself (Malik *et al.*, 1994; Rupprecht *et al.*, 1994). Comparatively, WT1 has been found to activate the promoters Amphiregulin (Lee *et al.*, 1999), Syndecane-1 (Cook *et al.*, 1996), and E-cadherin (Hosono *et al.*, 2000). The sheer number and variety of different gene classes regulated by WT1 further exemplify the importance of this protein in day to day cellular maintenance, and on a larger scale, implicate its potential involvement in a number of physiological processes and disease.

The notion that WT1 may play a multifunctional role in the cell, and may not only act as a classical transcription factor, was brought to light when WT1 was found to be associated with splicing factors in kidney cell lines and fetal tissues (Charlieu *et al.*, 1995). Soon after, WT1 was also found to associate with other proteins, such as p53 (Maheswaran *et al.*, 1993; Maheswaran *et al.*, 1995), par4 (Johnstone *et al.*, 1996) and Ciao 1 (Johnstone *et al.*, 1998). The ability of WT1 to act not only as a

transcription factor, but also its ability to associate with splicing factors and other proteins, further complicate the question of WT1 function, which is still under intense investigation.

1.2.6. WT1 involvement in post-translational processes

snRNPs and splicing factors are commonly found in two nuclear domains within the nucleus: regions that contain interchromatin granules which are visualized as 20-50 speckles and 1-5 coiled bodies (Nyman *et al.*, 1986; Spector *et al.*, 1991). Transcription factors on the other hand, such as Sp1, typically localize to areas of the nucleus that display a diffuse nuclear stain when observed under the fluorescence microscope.

The first evidence suggesting a role for WT1 in posttranslational processes came from the discovery that the +KTS and –KTS isoforms of WT1 colocalized in different regions of the nucleus (Larsson *et al.*, 1995). Staining techniques were used to show that WT1 was found within regions of the nucleus associated with transcription and to areas associated with snRNPs. It was found that this differential localization was somewhat dependant on the presence or absence of KTS in between zinc fingers 3 and 4.

In the above study, it was found that the +KTS isoform of WT1 is predominantly found within speckles/coiled bodies and co-immunopreciptates with splicing factors; whereas the –KTS isoform is found localized in large transcription factor domains as are other transcription factors that bind to DNA (Bickmore *et al.*, 1992; Drummond *et al.*, 1994).

By a combination of co-immunoprecipitation, yeast 2-hybrid, and splicing experiments, it was shown that WT1 interacts with the splicing factor U2AF65 (Davies *et al.*, 1998). Although both WT1 isoforms were able to interact with U2AF65, a yeast 2-hybrid assay demonstrated that the +KTS isoform exhibited a stronger interaction. Moreover, it was also demonstrated that WT1 could be incorporated into spliceosomes.

The hypothesis that WT1 is involved in post-transcriptional processes was further supported when WT1 was discovered to be present in nuclear poly(A)+ RNP particles (Ladomery *et al.*, 1999). It was becoming increasingly evident that WT1 could have many functions within the cell. Evidence suggested that WT1 was not only a transcription factor, but that it could also play a role in post-transcriptional processes such as RNA splicing.

The number of potential biological roles of WT1 were increased in 2004 when it was discovered that WT1 could shuttle between the nucleus and cytoplasm (Niksic *et al.*, 2004). In contrast with regions of localization, it was shown that both the –KTS and +KTS isoforms exhibit this ability to shuttle. Furthermore, WT1 was found to be associated with polyA RNPs within the cytoplasm and both isoforms were found to co-fractionate with actively translating polysomes (Niksic *et al.*, 2004). This observation extended the possible functions of the WT1 protein and demonstrated the critical need for further experiments into the biochemical role of this protein.

1.2.7. WT1 in development and disease

During mammalian embryological development, WT1 is expressed in many different tissue types such as the kidneys, spleen, heart, gonads, brain, spinal cord,

limbs and the mesothelial lining of abdominal organs (Wagner *et al.*, 2003). These tissue types all have one feature in common; their mesenchyme cells transform to epithelial cells during embryonic development (Lee and Haber, 2001). This finding indicates that WT1 perhaps is involved in, or responsible for, the initiation of mesenchyme transformation, and implicates WT1 in a variety of developmental abnormalities involving mesothelial tissues. Other studies have shown that WT1 is expressed in an even wider variety of tissues such as the stem cells of bone marrow, development of the retina, the septum transversum, the epicardium and the subepicardial mesenchyme (Discenza and Pelletier, 2004). The broad range of tissue types that express WT1 during development indicate its importance during embryogenesis.

1.2.8. WT1 and nephron differentiation

Early studies of WT1 indicated that it was involved in nephron and kidney development. The first clue came from the observation that WT1 is expressed in a specific pattern during development of the kidney. First, WT1 is expressed at a general low level in the beginning of metanephric development. It is then up regulated in the mesenchyme tissues as they differentiate into nephrons. Finally, WT1 expression increases again as glomerular podocytes form (Armstrong *et al.*, 1993).

Further evidence that WT1 is essential in renal development came from studies of WT1-/- mice. In these mice, cells that are supposed to develop into kidneys die via apoptosis, thus indicating that lack of WT1 disrupts renal development at its earliest stages (Kreidberg *et al.*, 1993). Furthermore, as previously discussed, specific mutations in WT1 lead to defects of glomerular maturation as observed in Denys-

Drash and Frasier syndromes (Little *et al.*, 1993; Little and Wells, 1997; Guo *et al.*, 2002).

These findings strongly indicated that action of WT1 is involved in glomerular maturation, but this was difficult to study further because WT1-/- mice die before glomerular maturation is reached. An elegant study carried out by Davies *et al.* in 2004, provided genetic evidence of WT1 function without the use of WT1-/- mice. They confirmed that the WT1 tumor suppressor was required for nephron differentiation using a newly developed siRNA-based method for repression of specific gene expression in kidneys grown in culture. When WT1 expression was knocked down after the point where nephron development fails in WT1-/- mice, development of the uteric bud was inhibited. Conversely, if WT1 is knocked down after the formation of the uteric bud, an unexpected phenomenon occurs where nephron formation ceases and is replaced by abnormal cell proliferation (Davies *et al.*, 2004). While it is too early to know whether the cells undergoing proliferation in culture correspond to those that give rise to Wilms' tumors, it is a potential connection and interesting line of study that should be investigated further.

1.2.9. WT1 and Cancer

Considering the vast array of tissues types that express WT1 during development and its role in cellular proliferation, it is not surprising that WT1 is involved in situations where proliferation has gone awry. Accordingly, WT1 has been found to be involved in many different cancer types. It is over expressed in almost all leukemias and also many solid tumors, such as breast, lung, prostate and colon cancer. In many cancer cases the WT1 gene is not mutated For example, the WT1

gene is mutated in only 13% of childhood leukemias. The mutations found were observed in the later stages of disease, suggesting WT1 mutation may play a role in the progression of leukemia (Miyagawa *et al.*, 1999; Oji *et al.*, 2004). A similar study indicated that wild type WT1 is involved in the formation of primary breast cancer tumors (Oji et al., 2004).

1.3. Nucleic acid binding by WT1

1.3.1. DNA Binding Activity

The first evidence that WT1 is a DNA binding protein came in 1990 when it was demonstrated that WT1 could bind to the core EGR-1 consensus sequence 5'-GCGGGGGCG-3' (Rauscher *et al.*, 1990). Only the –KTS isoform was able to bind to this DNA sequence.

Using a whole-genome PCR approach, a high affinity DNA binding site for WT1 (WTE) was identified to be 5'-GCGTGGGAGT-3'. Although the WTE site is similar to the consensus sequence recognized by EGR-1, WT1 has a 20-30 fold higher affinity for it compared to the EGR-1 binding motif. These experiments also demonstrated a clear role for zinc finger 1. Deletion or mutation of finger 1 abolished DNA binding by WT1 (Nakagama *et al.*, 1995).

In most studies the +KTS isoform has not been found to bind to DNA with high affinity. However, two potential DNA binding sites for the +KTS isoform have been identified; a region within the PDGF A- chain promoter (Wang *et al.*, 1995) within a unique G +C region and a DNA sequence refered to as + P5 (Bickmore *et al.*, 1992). Both isoforms bind to the +P5 site but not the PDGF-A site. Using zinc finger deletion mutants of WT1, Bickmore *et al.* showed that finger 1 but not finger 4

is critical for +P5 binding. In comparison finger 4, but not finger 1, is essential for the binding of WT1 to EGR1 and PDGF A chain promoters. This result is interesting because it conflicts with other studies done by Nakagama et al. (Nakagama *et al.*, 1995) which suggest that finger 1 is the most crucial finger involved in EGR1 consensus binding.

In order to fully investigate the DNA binding properties of the WT1 -KTS isoform, more rigorous quantitative studies were required. Data from crystallography studies of the EGR-1 (Zif268) protein bound to its nine base pair consensus sequence initiated new hypotheses as to the mode of WT1 DNA binding. With the knowledge that zinc fingers tend to contact a 3-4 base pair sub site of the DNA, and knowing that the last 3 fingers of WT1 have conserved base contacting residues with EGR1, it was thought that finger 1 of WT1 most likely occupies its own sub site on the DNA and that WT1 could bind to a 12 base pair sequence.

Using a binding site selection assay, Hamilton *et al.* (Hamilton *et al.*, 1995) investigated the role of finger 1 in WT1 binding, and also identified high affinity binding sites for WT1. Using zinc finger fusion proteins containing the zinc finger region of WT1 -KTS, they found that indeed WT1 recognizes a 12 base pair sequence. Using a quantitative nitrocellulose binding assay they found that the highest affinity binding site for WT1 -KTS was the 12 bp sequence 5'-GCG-TGG-GCG-(T/G)(G/A)(T/G)-3', and that a WT1 ZF fusion protein lacking the first zinc finger could only recognize the sequence 5'-GCG-TGG-GCG-3'. Further quantitative experiments found that WT1 -KTS has the highest affinity for the DNA binding site

5'-G(T/C)G-(T/G)GG-GAG-(T/C)G(T/C)-3' indicating that EGR1 and WT1 bind to different but related DNA sequences (Hamilton *et al.*, 1998).

1.3.2. RNA binding activity

It has been demonstrated that both the +KTS and –KTS isoforms of WT1 can bind to specific RNA sequences *in vitro* with binding being mediated through the zinc finger domain. The first evidence of this came from studies of a WT1 fusion protein containing only the zinc finger domain that could bind to a specific Igf-2 exonic RNA sequence (Caricasole *et al.*, 1996).

The zinc finger region of WT1 was also found to bind RNA ligands selected from a random RNA pool. Of the ligands studied, an aptamer designated clone 22 (to be referred to as Pel22 after the researcher who identified it) had the highest affinity for WT1 –KTS with a reported K_d of 0.7 μM. In this study +KTS demonstrated greatly reduced binding with the same aptamer in the same assay (Bardeesy and Pelletier, 1998). Subsequent investigation of the properties of WT1 binding with the aptamer designated by the Pelletier group as clone 22 (Pel22), showed that both –KTS and +KTS could bind to the aptamer with K_d values of 13.8 nM and 22.8 nM respectively (Zhai *et al.*, 2001).

The equilibrium binding of the WT1 zinc finger domain with the RNA aptamer Pel22 has been thoroughly investigated and compared with equilibrium binding of WT1 with DNA (Zhai *et al.*, 2001). The effects of changes in assay conditions such as pH, temperature and monovalent and divalent salt conditions can distinguish subtle differences in the nucleic acid binding properties of a protein. Experiments demonstrated that there are some similarities and some differences in

WT1-RNA and DNA binding. Both DNA and RNA interactions have the same dependence on temperature, and as the temperature increases the affinity of the protein for the nucleic acids increases indicating that both interactions are driven by entropy. Analysis of the monovalent salt dependence suggests that the formation of the WT1-DNA complex results in the release of more ions then are released during the formation of the WT1-RNA complex. Also, the binding of WT1 to DNA occurs over a broader pH range than WT1-RNA binding, which suggests that one or more titratable groups on WT1 or on Pel22 make significant contributions to the interaction.

An mfold program was used to predict the lowest-free energy forms of Pel22 which placed the consensus sequence on the 3' side of a hairpin stem loop structure (Zhai *et al.*, 2001). Mutational analysis of the Pel22 RNA was used to examine specific structural requirements for interaction with WT1. The most drastic decrease in affinity of Pel22 for WT1 was found when mutations were made in the non-consensus region of the RNA that altered the size of the hairpin loop. A similar decrease in affinity was seen for a mutant that had disrupted base pairing of the stem structure without altering the sequence or placement of the consensus sequence in the RNA. These results clearly demonstrate that nucleotides that are not in the consensus sequence are essential for WT1-RNA binding, and that the structure of the RNA, specifically the hairpin loop, is crucial for binding.

The discovery that +KTS does in fact bind to RNA *in vitro* supports the theory that WT1 +KTS is involved in RNA metabolism; however, there is ongoing disagreement as to which zinc finger is most crucial in RNA binding. Using a

qualitative gel shift assay (Caricasole *et al.*, 1996) it was shown that RNA binding was abolished when finger 1 was removed, while a WT1 mutant lacking finger 4 still retained some RNA binding capabilities. In contrast, the same group that identified the RNA aptamers to which WT1 binds found that WT1 mutants lacking finger 1 retained RNA binding, whereas mutants that lacked finger 4 bound poorly to RNA (Bardeesy and Pelletier, 1998).

This confusion over which zinc fingers of WT1 are involved in RNA binding is ongoing. Common to all of these studies is the use of qualitative RNA binding assays. Conclusions have been based on the result of single point gel mobility shift assays. Also, it must be kept in mind that full deletion of a zinc finger could potentially alter the stability of the protein and cause it to bind in a different manner. It is therefore important to validate or refute these findings first in a quantitative manner, and second in a way that attempts to control for altered protein stability.

1.4. Introduction to this study

It is evident that the mechanism by which WT1 interacts with RNA remains to be elucidated. Conflicting results point to different zinc fingers as the most crucial for RNA binding activity. The purpose of this study was to use site directed mutagenesis and deletion mutants to probe the mechanism of RNA binding by WT1. In order to improve on previous qualitative studies, binding dissociation constants were determined using a quantitative nitrocellulose filter binding assay that has been used previously by our laboratory (Romaniuk, 1985; Romaniuk *et al.*, 1989; Romaniuk, 1990; Zang and Romaniuk, 1995; Hamilton *et al.*, 2001; Zhai *et al.*, 2001).

By creating mutations within the zinc finger regions, it was possible to observe differences in binding affinities without having to make large deletions that could potentially alter the tertiary structure of the protein. Experiments were designed so that if a region of a zinc finger (or zinc fingers) is important for RNA binding, this would be observed as a decreased binding affinity for RNA by the mutant protein within the context of a properly folded zinc finger domain.

On the small scale, this study attempted to determine which individual zinc finger (or fingers) are most vital for RNA binding. Results of this study may in turn give rise to other studies that will impart further insight into the role of this tumor suppressor protein in normal cellular processes and tumorigenesis.

Chapter 2. Methods and Materials

2.1. Vector Plasmids containing cDNA of wild type and mutants

2.1.1. Wild type WT1 and control plasmid constructs

A cDNA encoding finger 4-7 of TFIIIA (TFIIIA4-7) cloned into the pRK172 expression vector was kindly given to our lab by Dr. Gottesfeld (Scripps) and the following cDNAs were provided by Dr. Romaniuk cloned into various plasmid vectors: the cDNA of WT1 cloned into pUC18 (Hamilton *et al.*, 1995), cDNA encoding the wild type zinc finger region of WT1 +KTS and -KTS cloned into the expression vector pET16b (Novagen), and p43 zinc fingers 1-4 and 6-9 cloned into the expression vector pET30a (Novagen). Both pET16b and pET30a encode a N-terminal 6XHIS fusion tag.

2.1.2. TFIIIA swap mutants (Wx)

The two mutants Wx1B+ and Wx2B+ cloned into the vector pCRT7/NT-TOPO (Invitrogen) were provided by Dr. Romaniuk. For expression of gene products, Wx1B+ and Wx2B+ were cloned in frame into the open reading frame of the TOPO vector pET 100/D TOPO (Invitrogen), whereas the mutants Wx3B+ and Wx4B+ were cloned in frame into the open reading frame of the pET30a vector (Novagen). All of the mutants were cloned in frame with a N- terminal 6XHIS fusion tag encoded by the vector pET 100/D TOPO and pET30a vectors respectively.

2.1.3. p43 6-9 swap mutants

All p43 swap mutants were cloned in frame into the expression vector pET30a. The mutant W12P8W4 was kindly cloned and provided by Dr. Romaniuk.

2.2. Mutant construction by site directed mutagenesis

2.2.1. Wx TFIIIA swap mutants

Four zinc finger mutants were constructed using mutagenic PCR. Each mutant was constructed so that one zinc finger was substituted within the α helical region with the corresponding sequence from a TFIIIA α helix (Figure 7). The mutants were designated Wx1B+, Wx2B+, Wx3B+ and Wx4B+, referring to which WT1 zinc finger α helix was replaced. Wx1B+ had the α helical region of WT1 finger 1 replaced with the α helical region from finger 4 of TFIIIA, Wx2B+ had the α helical region of WT1 finger 2 replaced with the α helical region from finger 5 of TFIIIA, Wx3B+ had the α helical region of WT1 finger 3 replaced with the α helical region from finger 6 of TFIIIA and Wx4B+ had the α helical region of WT1 finger 4 replaced with the α helical region from finger 7 of TFIIIA. The template that was used to create the mutants was the plasmid pUC18WT1(KTS)ZF, which contains the zinc finger domain of WT1(KTS) cloned into pUC18 (Hamilton *et al.*, 1995) and the mutagenic primers were developed by Dr. Romaniuk (Table 2). Two different methods of PCR were employed to construct the four swap mutants. Wx1B+ and Wx2B+ were constructed using the mutagenic primers listed in Table 2. These mutants were made by Dr. Paul Romaniuk, by a method described before

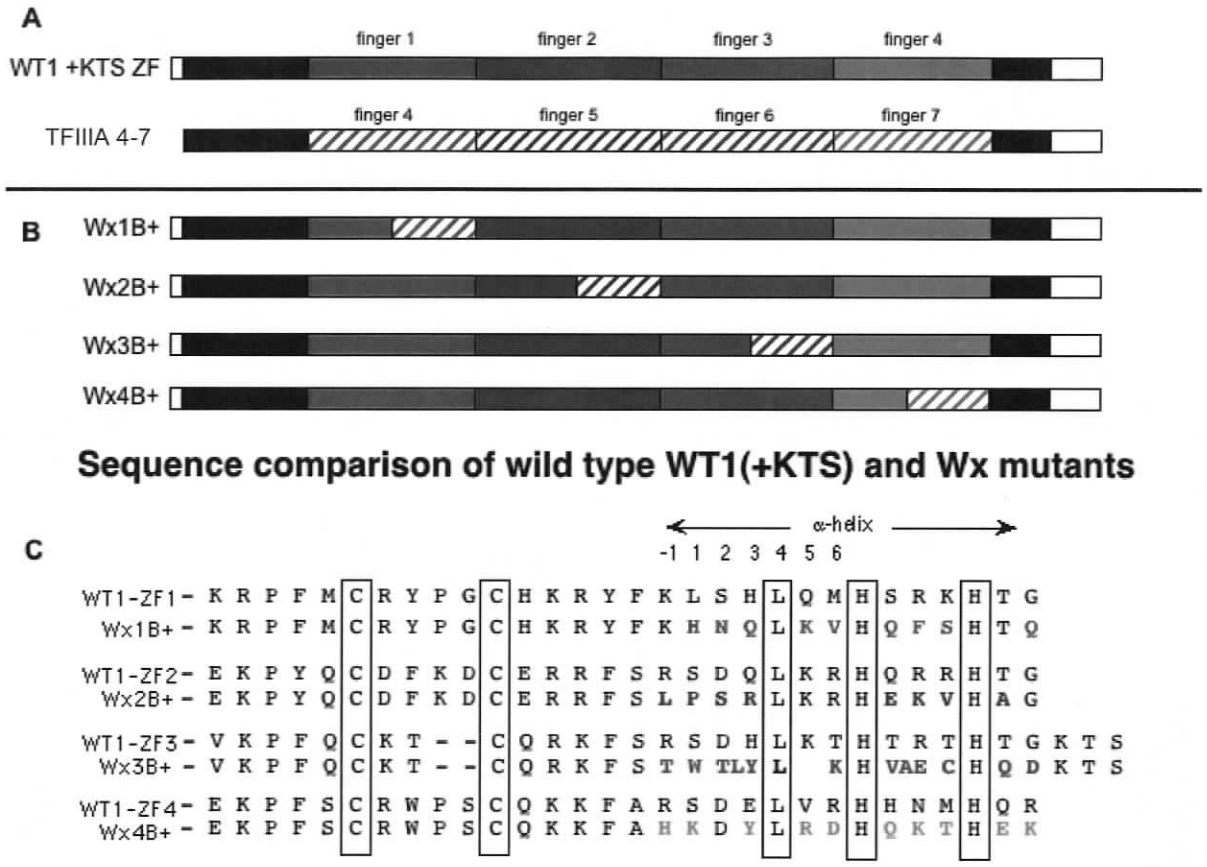

Figure 7. Top: A Schematic diagram of the WT1(+KTS) and Wx+ zinc finger domain cDNA's that were created by finger swapping mutagenesis using TFIIIA zinc fingers as donor templates. Hatched regions represent cDNA originating from TFIIIA 4-7. Bottom: A comparison of the amino acid sequences of wild type WT1 zinc fingers and the Wx+ mutant zinc fingers. Residues that are required for zinc finger folding are boxed, and amino acid changes are depicted in colour. Red amino acids originate from TFIIIA finger 4, blue amino acids originate from TFIIIA finger 5, green amino acids originate from TFIIIA finger 6 and orange amino acids originate from TFIIIA finger 7.

(Dillon and Rosen, 1990), and were kindly given to me cloned into the plasmid pCRT7/NT-TOPO (Invitrogen).

2.2.1.1. Wx3B+ and Wx4B+

The WT1 mutants Wx3B+ and Wx4B+ were constructed using a different method of PCR. In this type of mutagenic PCR, two PCR products are produced that have an over-lapping sequence either upstream or downstream of the mutated region (Fig 9). A final round of amplification is then done using the two PCR products as templates to produce a full length DNA that contains the introduced mutation. The mutagenic PCR of Wx4B+ was done by Megumi Tackiguchi and was given to me as a purified PCR product.

2.2.1.2. Site directed mutagenic PCR to create the swap mutant Wx3B+

The Wx3B+ swap mutant was constructed in three steps (Fig 9). In mutagenic PCR-1, a 20 µl reaction was set up containing 0.3mM dNTP's (dATP, dCTP, dGTP, dTTP), 1 mM $MgSO_4$, 1ng of the template pUC19WT1KTSZF linearised with SmaI, 0.5 units of Platinum Pfx DNA Polymerase (Invitrogen) and 2X Platinum Pfx amplification buffer (Invitrogen). PCR-1 contained a final concentration of 0.3 µM downstream mutagenic primer 3xB+ (5'CGAAAGTTCAAGACGTGGACCCTC TATCTTAAGCACGTCGCCGAGTGTCATCAAGATGAAAAGCCCTTC-3') and 0.3µM upstream primer FUP (5'- GTTTTCCCAGTCACGAC-3'). The DNA was amplified in a Biometra T personal thermocycler with an initial denaturation at 94°C

Table 2. Primers used in the construction of WT1 swap mutants. Underlined codons arise from TFIIIA cDNA and encode amino acids derived from TFIIIA.

Mutant name	Zinc finger substitution	Sequence of primer
Wx1B+	1	AAG AGA TAT AAA AAG CAT AAC CAG CTG AAG GTG CAC CAG TTC AGC CAC ACT CAA GAG AAA CCA TAC
Wx2B+	2	AGG TTT TCT CTT CCA TCC CGG CTT AAG AGA CAC GAA AAG GTA CAT GCA GGT GTG AAA CCA
Wx3B+	3	CGA AAG TTC AAG ACG TGG ACC CTC TAT CTT AAG CAC GTC GCC GAG TGT CAT CAA GAT GAA AAG CCC TTC
Wx4B+	4	AAA AAG TTT CGC CAT AAA GAT TAC TTA AGG GAC CAT CAA AAG ACG CAT GAG AAA AAC ATG ACC

for 5 minutes, and 35 cycles with denaturation at 94°C for 10 seconds, annealing at 55°C for 10 seconds, and an extension at 68°C for 60 seconds. A final extension was then carried out at 68°C for 2 minutes. The 253bp product from this reaction was purified using a QIAquick column (Qiagen) following the PCR purification procedure outlined in the QIAquick Spin Handbook (Qiagen, 2002).

In mutagenic PCR-2, another 20 µl reaction was set up under the same general conditions as PCR-1, except it contained 0.3 µM upstream Wx3B+ down primer (5'-GCTTAAGATAGAGGGTCCACGTCTTGAACTTTCGCTGACAAG-3') and 0.3 µM RUP downstream primer (5'- CAGGAAACAGCTATGAC-3'). The DNA was amplified using the same cycle as the PCR-1 reaction. The 276 bp product was purified using a QIAquick column (Qiagen) following the PCR purification procedure outlined in the QIAquick Spin Handbook (Qiagen, 2002)

In order to generate a full length, mutated Wx3B+ cDNA, a final round of PCR (PCR-FINAL) was set up using 1µl of PCR-1 and 1µl of PCR-2 products as templates. These two PCR products have an overlap of 24bp at the 3'end of PCR-1 and the 5'end of PCR-2, so that they can anneal to allow for a full length PCR product to be amplified. The 20 µl PCR reaction contained 1 mM $MgSO_4$, 2X Pfx Amplification buffer (Invitrogen), 0.5 units of Platinum Pfx Polymerase (Invitrogen) and 0.3 µM of the up WT1 Nco primer (5- CGTTCACCATGGGAC GTGTGCCTGG-3') and 0.3 µM of the down WT1 Eco primer (5'-CAGTCC GAATTCCTATCAAAGCGCCAGCTGGAG-3'). The DNA was amplified in the thermocycler previously described, with an initial denaturation at 94°C for 5 minutes, 35 cycles at 94°C for 30 seconds, 55°C for 30 seconds and 68°C for 1 minute and 30

seconds, and then a final extension of 2 minutes at 68°C. The 462 bp PCR product was again purified using a QIAquick column (Qiagen) as described above.

2.2.2. p43 swap mutants

The four Wp mutants Wp1, Wp1-2, Wp3-4 and Wp4 (Figure 8) were created by site directed mutagenesis. Each mutant was created in 3 separate PCR steps (Figure 9). PCR-1 used a mutagenic primer that was specific for wild type WT1 cDNA, but had between 4-6 nucleotides corresponding to p43 6-9 cDNA at the 5' end. PCR-2 used a mutagenic primer that was specific for wild type p43 6-9 cDNA but had 15-22 nucleotides corresponding to wild type WT1 at the 3' end. The resulting products from these two PCR reactions had a region of overlap within the region where the zinc finger mutation junction between p43 6-9 cDNA and WT1 cDNA occurs. In PCR-FINAL both of the products from PCR-1 and PCR-2 were used as templates, and were designed to anneal at the overlapping junction and then be amplified to create a full length WT1 mutant cDNA with the corresponding p43 zinc finger swaps. The primers used in PCR-FINAL each contained a restriction enzyme site to be used in cloning of the mutants. The upstream primer contained an NcoI site and the downstream primer contained an EcoRI site.

The primers that were used for each of these PCR reactions are shown in Tables 3 through 5. The reactions were all set up with the same reagent concentrations as the mutagenic PCR used to construct the Wx3B+ mutant (2.2.1.2), and were amplified in the same thermalcycler under the same cycling conditions.

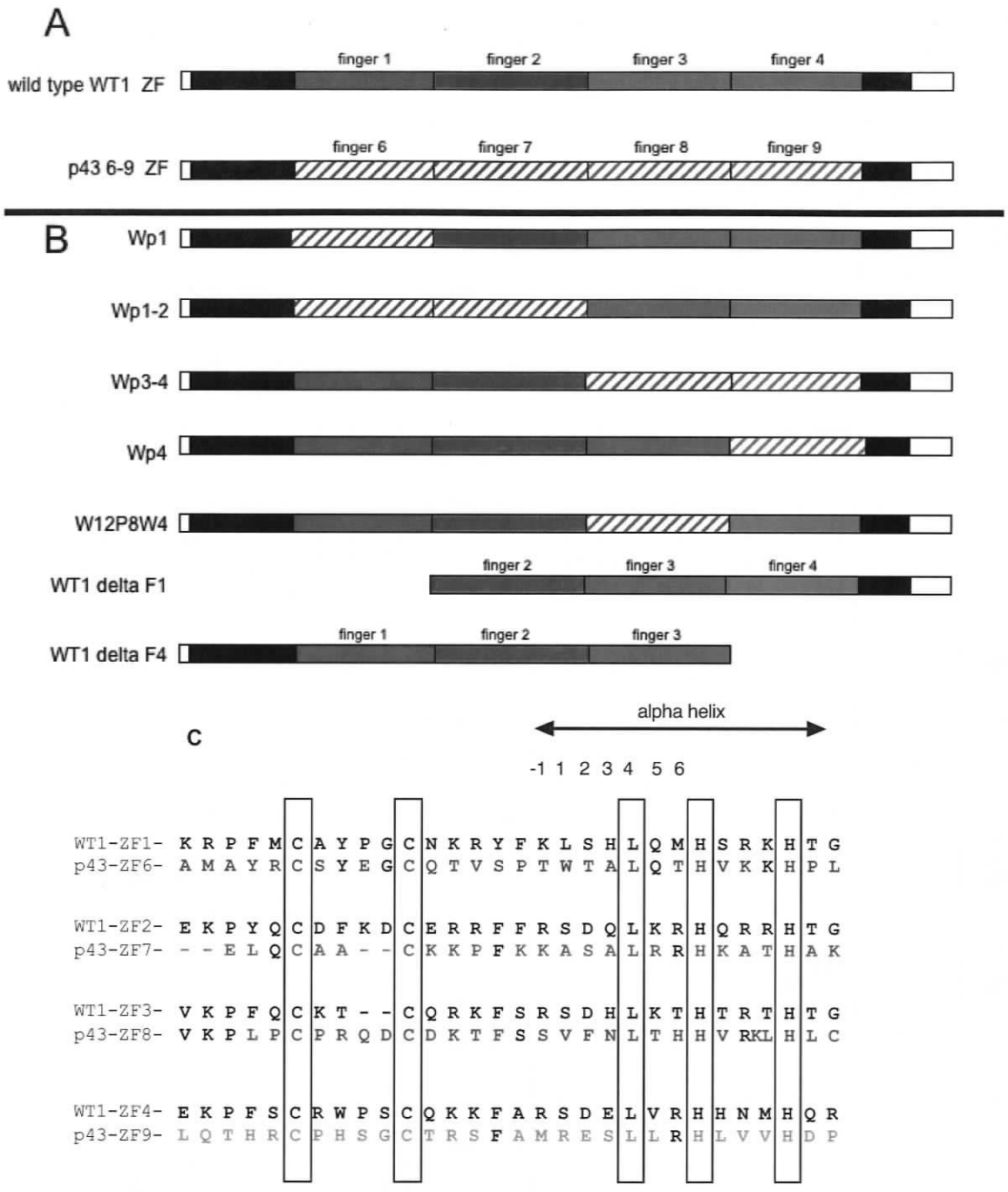

Figure 8. A. Diagram of Wild type WT1 –KTS and p43 6-9 constructs used to make swap and deletion mutants. B. Schematic diagram of p43 swap mutants and WT1 deletion mutants that were created by site directed mutagenic PCR, hatched regions originate from p43 6-9 cDNA. C. Diagram of amino acid changes in mutant fingers compared to wild type WT1. Residues that are required for zinc finger folding are boxed, and amino acid residues originating from p43 are depicted in colour: p43 F6 (blue), p43 F7 (red), p43 F8 (green), p43 F9 (orange).

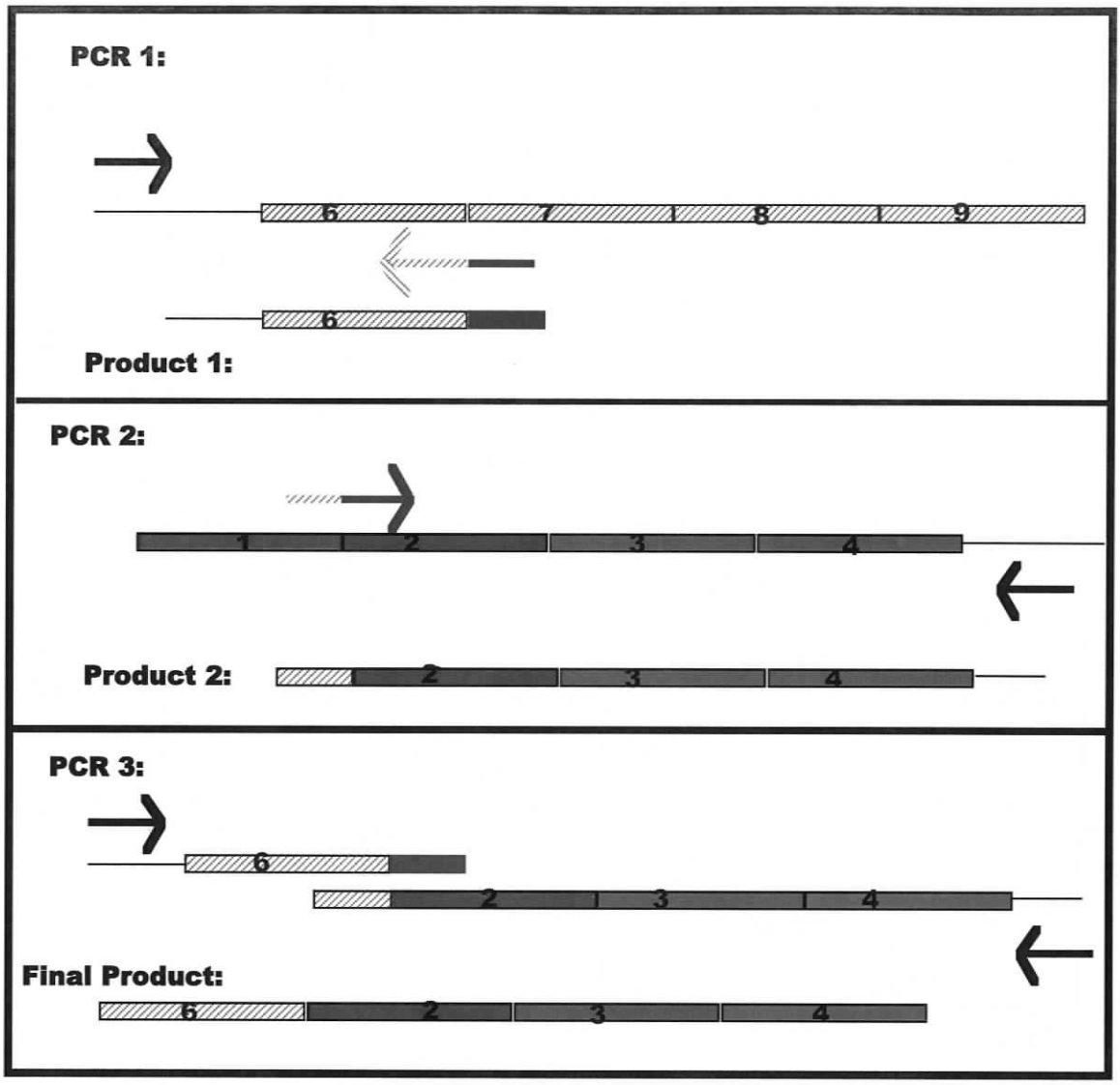

Figure 9. Schematic diagram indicating an example the 3-step reaction process that was used to generate the p43 swap mutant Wp1. The mutants Wp1-2, Wp3-4, Wp4 and Wx3B+ were created in a similar 3-step manner.

Table 3. Primer pairs used in PCR-1 to create the four swap mutants Wp1, Wp1-2 Wp3-4 and Wp4. Bold characters indicate sequences derived from p43 6-9 cDNA and underlined nucleotides indicate region of the primers that overlap with corresponding primer from PCR-2. RUP = 5'- CAGGAAACAGCTATGAC-3'. FUP = 5'-GTTTTCCCAGTCACGAC-3'.

PCR-1

Construct	Mutagenic primer		Up/Down primer
Wp1	WT1F2up	**5' c ttg** gag aaa cca tac cag tgt gac**-3'**	RUP
Wp1-2	WT1F3up	**5'-g aac** aaa cca ttc cag tgt aaa act tgt c-3'	RUP
Wp3-4	WT1F2down	**5'-ca ggg cag** tgg ttt cac acc tgt atg tct c**-3'**	FUP
Wp4	WT1F3down	5'-**gca gcg gtg** ggg ctt ttc act tgt ttt acc tg-3'	FUP

Table 4. Primers pairs used in PCR-2 to create the four swap mutants Wp1, Wp1-2 Wp3-4 and Wp4. Bold characters indicate sequences derived from p43 6-9 cDNA and underlined nucleotides indicate region of the primers that overlap with corresponding primer from PCR-1. RUP = 5'- CAGGAAACAGCTATGAC-3'. FUP = 5'-GTTTTCCCAGTCACGAC-3'.

PCR-2

Construct	Mutagenic primer		Up/Down primer
Wp1	Wp1down	5'-c aca ctg gta tgg ttt cac caa **ggg gtg ctt ctt tac g**-3'	FUP
Wp1-2	Wp1-2down	5'-gt ttt aca ctg gaa tgg ttt **ctt ctt ggc gtg ggt ggc**-3'	FUP
Wp3-4	Wp3-4up	5'-cat aca ggt gtg aaa cca **ctg ccc tgc ccc cgc cag gac-3'**	RUP
Wp4	Wp4up	5'gt aaa aca agt gaa aag ccc **cac cgc tgc ccc cac tcc ggc tgc ac-3'**	RUP

Table 5. Primers used in PCR-FINAL create the four swap mutants Wp1, Wp1-2 Wp3-4 and Wp4 and the two deletion mutants WT1Δ1 and WT1Δ4. The EcoRI primer was paired with the corresponding NcoI primer.

Final PCR

Construct	EcoRI primer	EcoRI Primer sequence
Wp1	WT1 Eco	CAGTCCGAATTCCTATCAAAGCGCCAGCTGGAG
Wp1-2	WT1 Eco	CAGTCCGAATTCCTATCAAAGCGCCAGCTGGAG
Wp3-4	P43F9Eco	GCAGCGGAATTCATTATCTTTCCGGATCATG
Wp4	P43F9Eco	GCAGCGGAATTCATTATCTTTCCGGATCATG
WT1Δ4	WT1F3Eco	CAGTCCGAATTCCTATCACTTTTCACCTGTATGAGTCC
WT1Δ1	WT1 Eco	CAGTCCGAATTCCTATCAAAGCGCCAGCTGGAG

Construct	NcoI primer	NcoI primer sequence
Wp1	P43F6 Nco	CGTTCACCATGGCGTACCGCTGCTCCTAC
Wp1-2	P43F6 Nco	CGTTCACCATGGCGTACCGCTGCTCCTAC
Wp3-4	WT1F1Nco	CGTTCACCATGGAGAAACGCCCCTTCATG
Wp4	WT1F1Nco	CGTTCACCATGGAGAAACGCCCCTTCATG
WT1Δ4	WT1F1Nco	CGTTCACCATGGAGAAACGCCCCTTCATG
WT1Δ1	WT1F2Nco	CGTTCACCATGGAGAAACCATACCAGTGTG

The mutagenic PCR of the mutant W12P8W4 was constructed in the same manner by Dr. Romaniuk.

2.2.3. WT1 deletion mutants

WT1 deletion mutants WT1Δ1 and WT1Δ4 were created in one PCR step using a primer that bound within the cDNA of WT1 either just upstream of finger 2 or just downstream of finger 3. Each primer contained an NcoI or EcoRI restriction enzyme site. The primer was then paired with a universal up or downstream primer designed to contain the other restriction enzyme site (Table 5), and amplified along side the mutants using the same cycles as in PCR-FINAL.

2.3. Cloning of PCR products

2.3.1. Cloning of Wx1b+ and Wx2b+ into pET 100/D-TOPO

As mentioned earlier, the mutants Wx1B+ and Wx2B+ were supplied by Dr. Romaniuk in the pCRT7/NT-TOPO vector. They were then linearized with the enzyme EcoRI. Each mutant was linearized in a 20 µl restriction digest reaction containing 1 µg of plasmid, 5 units of EcoRI (New England Biolabs), and 2 µl of 10X buffer H to a final concentration of 5mM NaCl, 10 mMTris-HCl, 1 mM $MgCl_2$, and 0.0025% Triton X-100, at pH 7.5 @ 25°C (New England Biolabs). The linearized plasmids were used as PCR templates to produce blunt ended products for use with the TOPO cloning kit (Invitrogen). Each 20 µl reaction was prepared with 1µl of a 1 in 100 dilution (final concentration ~10-50 ng/µl) of either linearized pCRT7/NT-TOPO-Wx1b+ or pCRT7/NT-TOPO-Wx2b+ and the same concentrations of general

reagents described above for Pfx PCR reactions. The primers used were 0.3 μM TOPO-WT1 primer (5'-CACCATGCGACGTGTGCCTGG-3'), and 0.3 μM TOPO-UMP primer (5'-GCGCGTGATCAGTACACGTGCC-3'). The reactions were amplified in the same thermocycler described earlier with an initial denaturation at 94°C for 1 minute, 60°C for 10 seconds, 68°C for 30 seconds and then 35 cycles at 94°C for 10 seconds, 60°C for 10 seconds, and 68°C for 30 seconds. The 563bp products were purified by methods described above.

The blunt end PCR products were cloned into pET 100/ D-TOPO (Invitrogen) following the procedures outlined in the Champion pET Directional TOPO Expression Kits, Version F (Invitrogen, 2003). Each reaction contained 1 μl of fresh PCR product, 1 μl of salt solution, 2 μl sterile water, and 0.5 μl of pET 100/D-TOPO vector. The reaction mix was incubated at room temperature for 30 minutes. The TOPO cloning reactions were then used to transform competent One Shot TOP10 cells (Invitrogen). 6 μl of the TOPO cloning reaction was added to one vial of One Shot TOP10 competent cells and incubated on ice for 10 minutes. The cells were then heat shocked for 30 seconds at 42 °C and transferred immediately to ice. 250 μl of room temperature SOC medium was added and the cells were incubated for 1 hour at 37°C shaking at 250 rpm. The cells were then plated in 200 μl aliquots onto pre-warmed LB plates containing 50 μg/ml of ampicillin, and were incubated overnight at 37°C.

2.3.2. Cloning of Wx3B+ and Wx4B+ into pET30a

Both of the Wx3B+ and Wx4B+ PCR were designed to contain flanking NcoI and EcoRI restriction enzyme sites. This allows for directional cloning into the

vector pET30a, which also contains an EcoRI and NcoI sites within the multiple cloning region.

The Wx3b+ and Wx4B+ PCR products were digested in a double digest with EcoRI and NcoI. Each reaction contained 10 μl of purified PCR product, 20 units of EcoRI (NEB), 20 units of NcoI (NEB) and 1X EcoRI reaction buffer (final concentration of 5 mM NaCl, 10mM Tris-HCl, 10 mM $MgCl_2$, 0.0025% Triton X-100), and was incubated at 37°C for 3 hours. 2 μg of pET 30a was also digested under the same conditions.

The digested PCR products were cleaned up using QIAquick spin columns following the procedures outlined above. The entire pET30a digestion reaction was run on a 1% agarose gel and the linearized plasmid band was cut out and purified using a QiaQuick spin column following the gel extraction procedure outlined in the Qiaquick Spin Handbook (Qiagen, 2002)

The digested and purified PCR products were cloned into similarly digested pET30a using T4 DNA ligase (Invitrogen). Each 40 μl reaction contained approximately 40 ng of digested pET30a, approximately 500 ng of digested PCR product, 1 unit of T4 DNA ligase, and a 1X T4 DNA ligase buffer (50 mM Tris-HCl, 10 mM $MgCl_2$, 1 mM ATP, 1 mM DTT, 5% (w/v) poly-ethylene glycol-8000) and were incubated overnight at 16°C.

Each cloning reaction was subsequently used to transform *E. coli* DH5α competent cells. 100 μl of cells were added to 15 μl of ligation reaction and incubated on ice for 5 minutes. The cells were then heat shocked at 42°C for 2 minutes and incubated on ice again for°5 minutes. 900 μl of room temperature LB media was

added to the cells and then incubated at 37°C for 1 hour with shaking at 250rpm. The cells were then pelleted at 6000rpm in a Baxter Biofuge 13 table-top centrifuge and the supernatant discarded. The pellets were resuspended in 50 µl of LB media and plated onto LB agar plates containing 50µg/ml of Kanamycin antibiotic. The plates were incubated overnight at 37°C.

2.3.3. p43 swap mutants and WT1 deletion mutants

All of the p43 swap mutants and WT1 deletion mutants were cloned into the EcoRI and NcoI sites of pET 30a. The ligation reaction was set up in the same manner as for the ligations of Wx3B+ and Wx4B+ and clones were maintained in *E. coli* DH5α.

2.4. Screening of clones

2.4.1. Screening Wx1B+ and Wx2B+ clones by restriction enzyme digest

Approximately 10 TOP10F (Invitrogen) colonies that had been transformed with each ligation reaction (Wx1B+-pET30a and Wx2b+-pET30a) were picked and gown overnight in 5 ml LB containing 50 µg/ml ampicillin. The next day plasmid was extracted and purified from each culture using Qiaprep mini prep spin columns following the procedure outlined in the Qiaprep Miniprep Handbook (Qiagen, 2002). The mini-preps were screened for the correct zinc finger mutation by digestion at a restriction site unique within the corresponding introduced mutation.

The mutant Wx1B+ contains an extra PvuII site within the mutated region of the cDNA in comparison with wild type WT1(KTS)ZF. Approximately 100 ng of each purified plasmid DNA was digested with 8 µl of a pre-mix containing 40 units

of PvuII enzyme and 1X NEB buffer 2 to a final concentration of 10 mM NaCl, 5 mM Tris-HCl, 1 mM $MgCl_2$, and 0.1 mM DTT supplemented with 100 ug/ml BSA. The digests were incubated for approximately 3 hours at 37°C. In order to determine which plasmids contained positive clones, digested and undigested plasmid were run on 0.8% agarose gels to identify clones that produced the correct banding pattern.

The mutant Wx2B+-pET 100/D-TOPO contains a unique AflII site. Approximately 100 ng of each purified plasmid DNA was digested with 8 µl of a pre-mix containing 40 units of AflII enzyme and 1X NEB buffer 2 to a final concentration of 10 mM NaCl, 5 mM Tris-HCl, 1 mM $MgCl_2$,and 0.1 mM DTT supplemented with 100 µg/ml BSA. Each digest was analysed on a 0.8% agarose gel to identify clones that were linearized and produced a band of the correct size.

2.4.2. Further Screening of Wx1B+ and Wx2B+ by diagnostic PCR

Wx1B+ and Wx2B+ clones that appeared to include the restriction site indicative of the corresponding zinc finger mutation were further analyzed by PCR. Primers were used that primed just up and downstream of the pET100/D-TOPO cloning site. A PCR pre-mix was prepared containing 1X Taq DNA polymerase buffer (Invitriogen), 1.5 mM $MgCl_2$, 0.2 mM dNTP's, 10 units Taq DNA polymerase (Invitrogen), 0.5 µM UMP forward primer, and 0.5 µM Pet16-TWP reverse primer and 1 ng DNA of the mutants clones in question. Each PCR reaction subsequently contained 19 µl of pre-mix and 1 µl of template plasmid containing clones that passed the restriction enzyme diagnostic test (pET 100/D-TOPO). The reactions were then amplified with an initial denaturation at 94°C for 5 minutes, and then 30 cycles at 94°C for 10 seconds, 55°C for 10 seconds and 72°C for 30 seconds. Aliquots from

the PCR reaction were analyzed on a 1.5% agarose gel to check for the correct band size of 811 bp.

2.4.3. Screening for potential positive Wx3B+ and Wx4B+ clones by colony PCR

In order to check for colonies that contain a plasmid with an insert of the correct size, colony PCR was preformed on 8 randomly chosen Wx3B+ and 8 randomly chosen Wx4B+ DH5α ligation transformants. Each PCR reaction contained a template of 1 colony, and 10μl of a PCR mixture containing 1X Taq amplification buffer (Invitrogen), 1.5 mM $MgCl_2$, 0.1 mM dNTP's, 0.5 units of Taq DNA polymerase (Invitrogen), 0.3 μM of the primer WT1 Eco (CAGTCCGAATTCCTATCAAAGCGCCAGCTGGAG-3') and 0.3 μM of the primer WT1 Nco (5- CGTTCACCATGGGACGTGTGCCTGG-3'). Each reaction was then amplified with an initial denaturation at 94°C for 1 minute, and then 40 cycles at 94°C for 10 seconds, 55°C for 10 seconds, 72°C for 1 min. 5 μl of each PCR reaction was run on a 1.0% agarose gel to check for a PCR product of the correct size. Each tip that had been used to pick a colony was streaked on a plate containing LB media and 50 μg/ml kanamycin and incubated overnight. If a PCR reaction contained a product of the correct size, the corresponding colony was used to innoculate 5 ml of LB media containing 50 μg/ml of ampicilin and grown up overnight. The plasmids were then purified as described before, using a QIAprep mini prep spin column.

2.4.4. ScreeningWx3B+ and Wx4B+ clones by restriction enzyme digest

The Wx3B+ and Wx4B+ mutants also contain a unique AflII site. In order to confirm that the clones identified by colony PCR also contained the correct insert, an

AflII digest of the potential clones was completed as previously described for Wx2b+.

As an additional confirmation, an EcoRI/NcoI double digest was performed to confirm that the insert sequence within pET30a and to make sure that the insert is of the appropriate size. The clones that had passed both the colony PCR and AflII digestion check were further digested in a reaction that contained approximately 100ng of each plasmid clone, 1X EcoRI reaction buffer (final concentration of 5 mM NaCl, 10 mM Tris-HCl, 10 mM $MgCl_2$, 0.0025% Triton X-100), 0.5 units of EcoRI and 0.5 units of NcoI and was incubated at 37 C for 3 hours. The entire digest was run on a 1% agarose to confirm correct product size.

2.4.5. Screening of p43 swap and WT1 deletion mutants

Colonies were screened for plasmids with inserts of the correct size by colony PCR and EcoRI/NcoI restriction enzyme digests as described above. PCR reactions and digests were set up under the same conditions as described previously.

2.4.6. Sequencing

Clones that passed all diagnostic tests were verified by direct di-deoxy DNA sequencing by the CBR sequencing facility at the University of Victoria. Only clones with the correct sequence were used to express protein.

2.5. Protein expression and purification

2.5.1. Wild type WT1 and mutants

The expression and purification of wild type WT1 and the mutants was carried out following a modified lab protocol. *E. coli* BL21 (DE3) competent cells (mutants) or *E. coli* BL21(DE3) PLysS (wild type) were transformed with 50ng of plasmid DNA containing the correct construct following the same transformation protocol as described earlier.

The cells were plated on LB plates containing 50 μg/ml of ampicillin (pET 16b and pET 100/D-TOPO) or kanamycin (pET30a) and incubated for 16 hours at 37°C. The following day, a single colony from each transformation was inoculated into 5ml of LB medium containing 50 μg/ml of the appropriate antibiotic and grown up overnight at 37°C with shaking at 250rpm. The next day, the overnight cultures were sub-cultured into 250 ml of LB medium containing 50 μg/ml of the appropriate antibiotic and grown up to log phase. Once an OD_{600} between 0.4 and 0.8 was reached, the cells were induced by the addition of isopropyl-β-D-thiogalactopyranoside (IPTG) to a final concentration of 1mM. The cells were harvested 6 hours later by centrifugation at 5000 rpm in a Beckman JA-16.250 rotor. The cell pellets were washed with 10 ml of buffer A (10mM Tris-HCl, pH 7.5, 5mM $MgCl_2$, 250 mM NaCl, 10 mM PMSF, 10% glycerol, 5mM DTT, 5mM imidazole), then resuspended in 20 ml of the same buffer and lysed using a French pressure cell (3 x for each culture). Cell debris was then pelleted by centrifugation at 15,000 rpm for 15 minutes in a Beckman JA-20 rotor. The supernatant was discarded and the cell pellet was re-suspended in 5 ml of buffer B (the same as buffer A plus 5 M urea), and

rotated for 16 hours at 4°C. The following day the crude lysate was pelleted again at 15, 000 rpm for 15 minutes and the supernatant was applied to a 1.5 ml nickel chelate column (BioRad). The column was washed twice, once with 5 ml buffer B, and then again with 2 ml of buffer B containing 50mM imidazole. The protein was eluted with 1 ml of buffer B containing 200 mM imidazole and 1ml of buffer B containing 300 mM imidazole and was collected in approximately 0.5 ml fractions. The protein concentration of each fraction was determined using Bradford Protein Assay Reagent (Biorad) with BSA as a standard, following the method outlined in the BioRad Protein Assay Handbook. The purified proteins were checked for purity and size by running the column fractions on a 15% SDS-page gel.

2.5.2. Purification of the protein TFIIIA4-7

A protein containing zinc fingers 4-7 of TFIIIA (TFIIIA4-7) was purified using a heparin/sepharose CL-6B column (Pharmacia), following a lab protocol. A 100ml culture was inoculated with 1ml of an overnight culture of BL21(DE#) PlysS cells containing 50μg/ml ampicillin that had been transformed by plasmid pRK172 containing the cDNA for TFIIIA4-7, and grown until an OD of 0.5 at 600nm was reached. $ZnSO_4$ (0.05 mM) was added and the cells were induced with IPTG. The cells were grown up for 4 hours and pelleted at 5000 RPM in a Beckman JA-16.250 rotor. The cells were resuspended in 4 ml ZF buffer (50 mM Tris-HCL pH 7.5 @ 4°C, 100 mM NaCl, 50 μM $ZnCl_2$, 10% glycerol, and 5 mM DTT) and lysed using a french pressure cell (3X throughput). The lysed cells were then pelleted at 10,000 rpm in a Beckman JA-20 rotor, and the supernatant discarded. The inclusion body pellet was then resuspended in 3 ml of ZF buffer + 5 M urea and rotated for 1 hour at

4 °C. After centrifugation at 10,000 rpm in a Beckman JA-20 rotor, the supernatant was loaded onto a 0.5 ml heparin/sepharose CL-6B column and the protein was eluted with 1ml fractions of ZF + 5M urea solutions containing increasing concentrations of NaCl (400 mM, 600 mM, 800 mM and finally 1 M). The proteins were checked for purity and size on a 15% SDS-page gel.

2.5.3. p43 1-4 and 6-9

The proteins p43 1-4 and p43 6-9 were purified by Tristen Weiss as part of her Masters project. She kindly provided these to me for use in my experiments.

2.6. *In vitro* RNA transcription and radiolabeling by run off transcription

Pel22 RNA and 5S RNAwere transcribed and radiolabeled *in vitro* using the MAXIscript In Vitro Transcription Kit (Ambion). The Pel22 template DNA contained the Pel22 sequence cloned downstream of the T7 promoter within plasmid PK18. The template was linearized downstream of the Pel22 sequence using the restriction enzyme RsaI. The 5S RNA template DNA contained the 5S RNA gene cloned downstream of the T7 promoter of pUC18 (Romaniuk *et al.*, 1987) and was similarly linearized just downstream of the 5S gene using the restriction enzyme DraI.

20 µl transcription reactions were set up containing 1 µg of linearized template DNA, 1X transcription buffer (Ambion), 0.5 mM of the nucleotides ATP, CTP and GTP, 0.025 mM of the nucleotide UTP, 2 µl of α-^{32}P UTP (800 Ci/mmol, Amersham), and 2 µl of T7 enzyme mix (Ambion). The reaction was incubated at 37°C for 1.5 hours and electrophoresed on an 8.3 M urea 8% acrylamide 1 X TBE

gel. The gel was exposed to film (BioMAX MR film, Kodak) for 3 minutes and developed on a Kodak X-OMAT 2000A Processor. The corresponding radiolabeled bands were cut out and eluted overnight at room temperature in 250 µl of RNA elution buffer (1 mM EDTA, 0.6 M NH_4OAC, 0.1% SDS). The following day the RNA was precipitated by adding 625 µl of ethanol and 1.5 µg glycogen to the elution buffer and incubated at -70°C for 1 hour. The samples were then centrifuged at 13, 000 rpm for 20 minutes in an Ependorf microcentrifuge, and the supernatant was decanted. The pellet was dried in a Savant speed vacuum concentrator and re-suspended in 100µl nuclease free water (Gibco). The radioactivity of the RNA was measured in a 1214 Rackbeta liquid scintillation counter in counts per minute (cpm).

2.7. Nitrocellulose filter binding assays

Proteins were diluted in the standard binding buffer TMK, which contained 20 mM Tris-HCl , 100mM KCl, 100µg/ml BSA, 1mM DTT, 5µM $ZnCl_2$, and either 1mM (WT1 and mutants) or 5mM MgCl2 (TFIIIA4-7). Proteins were serially diluted to concentrations of 1-800nm in a final volume of 80µl TMK buffer. The assay was started by the addition of ^{32}P labeled RNA with a total of 5000 cpm per reaction (pM range) containing 0.5 µg poly dI-dC (Sigma) in 20 µl TMK buffer. The reactions were equilibrated for 1.5 hours at room temperature and 80 µl aliquots were vacuum filtered through a pre-soaked 0.45 µm nitrocellulose membrane using a dot-blot apparatus. The filter was then dried and exposed to a Molecular Dynamics phosphor screen for a minimum of 4 hours and visualized using STORM imaging system

The nitrocellulose membrane retains only protein while RNA passes through, therefore the relative radioactivity on the membrane represents only RNA that is in

complex with protein. The apparent dissociation constants for binding of the mutant and wild type proteins were determined by fitting the data to the simple bimolecular equilibrium equation:

$$K_d = \frac{[\text{Protein}]_{free}[\text{RNA}]_{free}}{[\text{Protein}\bullet\text{RNA}]_{complex}}$$

where in this case, $[\text{Protein}]_{total} = [\text{Protein}]_{free}$ because the concentration of the protein-RNA complex is negligible in comparison to free protein concentration.

The filter binding assay can be used to determine the binding dissociation constant of a protein RNA complex as long as two main assumptions are made. Incomplete retention on nitrocellulose filters is a known phenomenon, and in this case we are assuming that the percentage of RNA bound at the plateau of the graph is representative of the complete binding of RNA molecules to WT1 and that the retention efficiency (percent retention of protein on the nitrocellulose) is constant for all protein concentrations tested (Carey and Uhlenbeck, 1983; Romaniuk, 1990). The other assumption that is being made is that each protein fraction is 100% active.

An equilibrium binding curve was obtained using Kaleidagraph software (Synergy Software, Reading, PA) by plotting the fraction of RNA bound against total protein concentration, where fraction of RNA bound = $[\text{protein}]_{total}/K_d + [\text{protein}]_{total}$. The apparent dissociation constant for each protein was determined from the curve generated, where K_d is equal to the protein concentration when 50% of the RNA is bound. Each equilibrium binding curve was carried out in triplicate, and the plots are representative of the average of 3 independent experiments.

Chapter 3. Results

3.1. Probing WT1 RNA interactions by using TFIIIA swap mutants

3.1.1. Overview

The RNA binding activity of the nine-zinc finger transcription factor TFIIIA has been extensively characterized *in vitro* (Clemens *et al.*, 1993; Hamilton *et al.*, 1995). The recently solved crystal structure of TFIIIA zinc fingers 4-6 complexed with a truncated version of its ligand 5S RNA (Lu *et al.*, 2003) has given us many insights into zinc finger-RNA recognition. As with DNA binding interactions, it appears as though zinc fingers form interactions with the RNA backbone and bases through key α-helix residues.

In order to try and understand how WT1 interacts with RNA, and to determine which α helix plays the most crucial role in WT1-RNA binding, WT1 finger swap mutants were constructed. The donor finger sequences used in this study originate from the cDNA of zinc fingers 4-7 of TFIIIA, which have vastly different sequences compared to WT1. Each mutant was created so that 1 α helix within a zinc finger is replaced with the α helix from the corresponding zinc finger of TFIIIA 4-7 (Figure 7).

3.1.2. Basis for using TFIIIA zinc fingers 4-7 as α helix donors

In 2001, Hamilton *et al.* investigated the RNA binding activities of the zinc finger protein TFIIIA. In one experiment, the zinc fingers 4-7 of TFIIIA were replaced with the 4 zinc fingers of WT1. This mutant TFIIIA construct (Xw4-7) was

no longer able to bind to 5S RNA. It also acquired the ability to bind to the high affinity RNA ligand of WT1 (Figure 10) which is aptamer clone #22 discovered in 1998 by Bardeesy and Pelletier (from now on this RNA aptamer will be referred to as Pel22).

3.1.3. Secondary structure comparison of Pel22 and 5S RNA

The secondary structures of Pel22 and 5S RNA are distinct. A mfold program was used to predict the lowest-free energy structure of Pel22 RNA (Zhai *et al.*, 2001). This sequence and secondary structure of Pel22 is very different from that of 5S RNA (Figure 12).

The differences in structure of these two RNA molecules further supported the notion that TFIIIA zinc fingers 4-7 would be sufficient donor sequences for making WT1 mutants; WT1 is specific for Pel22, TFIIIA is specific for 5S RNA, and there isn't a high degree of sequence or structural homology between the two RNA ligands.

3.1.4. Using finger swap mutants to probe the WT1-RNA interaction

Romaniuk's group has previously demonstrated that both the –KTS and +KTS isoforms of WT1 can bind to the RNA aptamer Pel22 with K_d values of 13.8 nM and 22.8nM respectively, and that neither isoform can bind to the TFIIIA ligand 5S RNA (Zhai *et al.*, 2001). The findings that WT1 cannot bind to 5S RNA, and that the TFIIIA mutant Xw4-7 has a binding specificity reversal from 5S RNA to Pel22 RNA, led us to hypothesize that we could use TFIIIA zinc fingers 4-7 as donor sequences to create WT1 mutants for use in identifying RNA binding determinants. It was thought

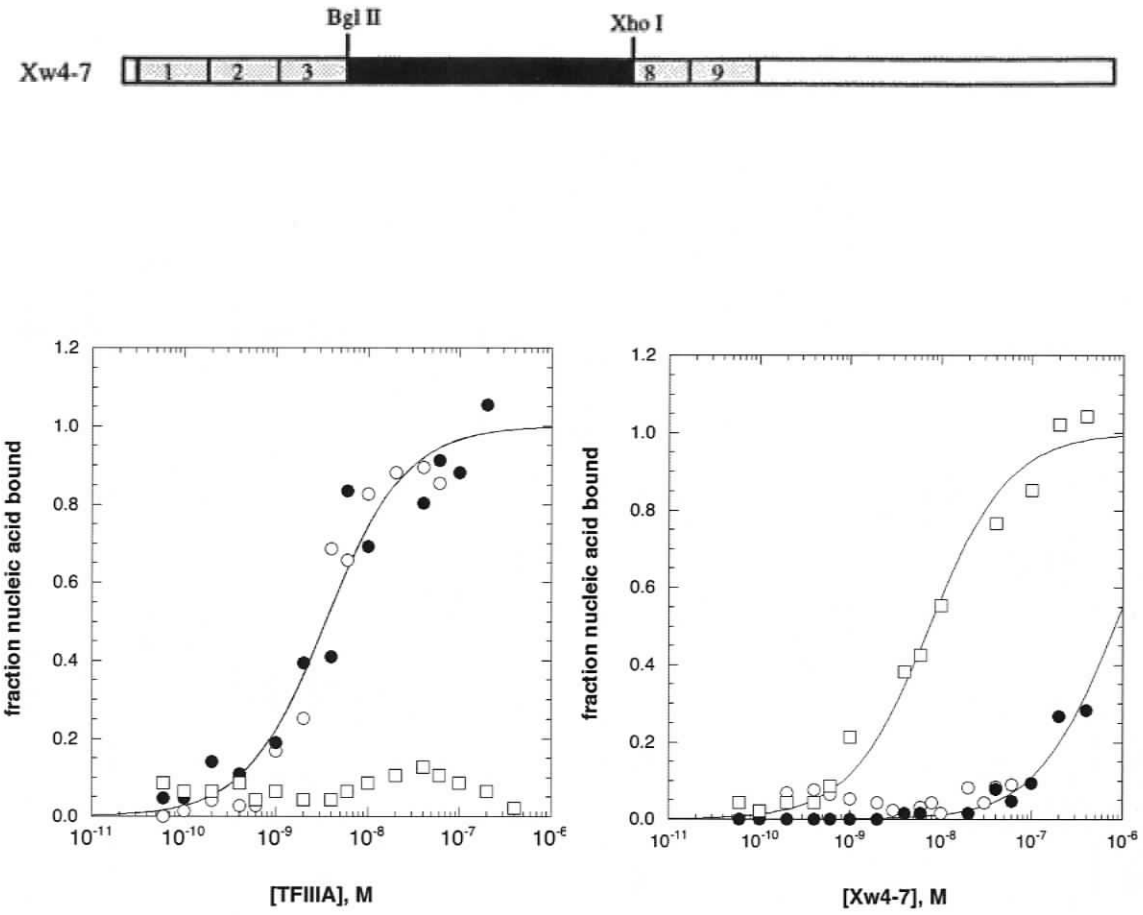

Figure 10. . Top. Schematic diagram representing the TFIIIA mutant (Xw4-7) that has fingers 4-7 replaced with the 4 fingers from WT1.Bottom. Equilibrium binding of wild type TFIIIA (left) and equilibrium binding of TFIIIA mutant Xw4-7 (right) to 5S DNA (○), 5S RNA (●), and Pel22 (□). The data are from a single nitrocellulose filter-binding assay and curves are best fit to a simple bimolecular equilibrium (Hamilton *et al.*, 2001).

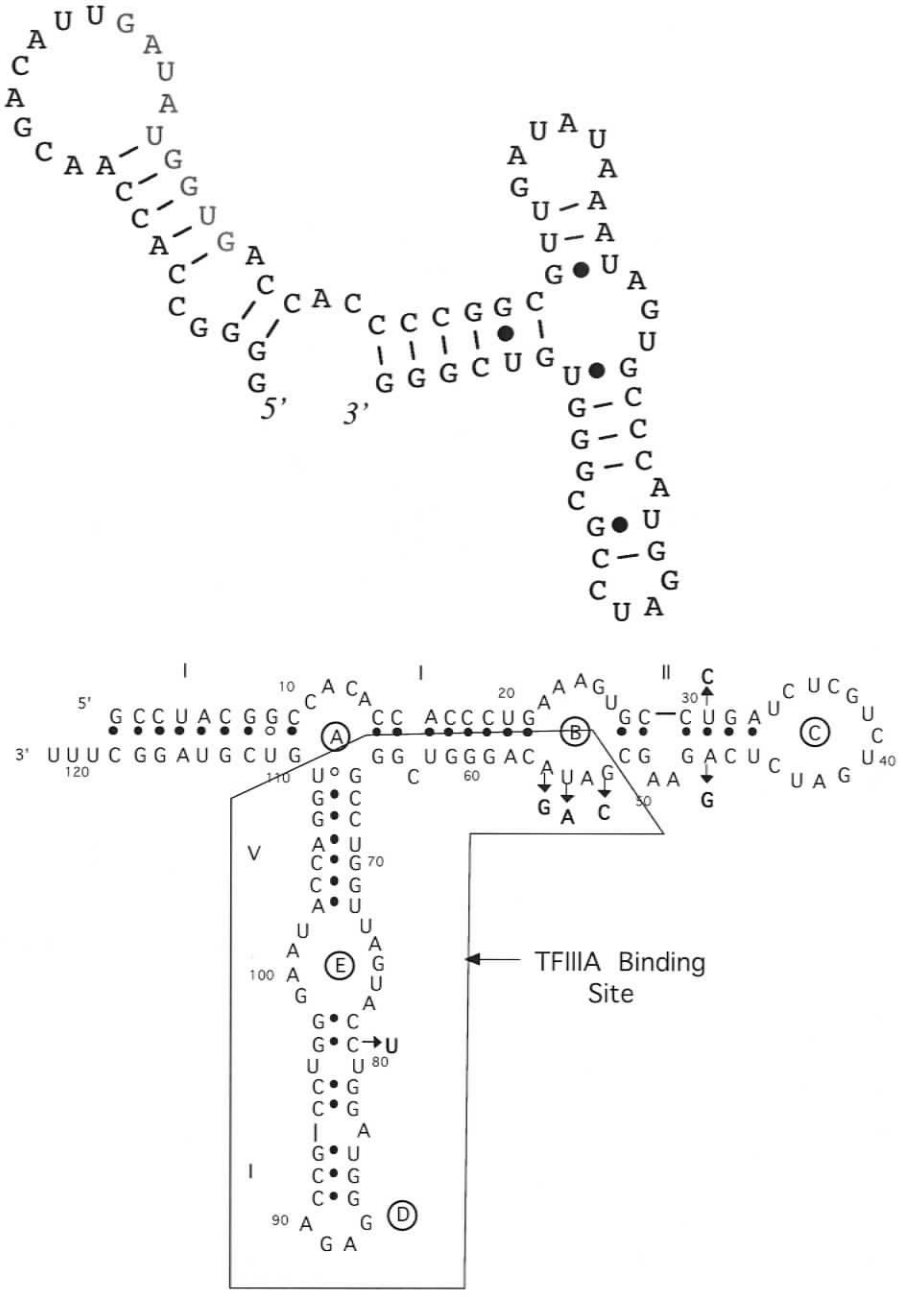

Figure 11. Top. Lowest-free energy structure predicted for Pel22, as determined by the mfold program (Zhai *et al.*, 2001). The consensus sequence is indicated in red letters. Bottom. Secondary structure of oocyte-type 5S RNA. Arrows indicate base changes in somatic-type 5S RNA. Box indicates TFIIIA binding site as determined by RNase footprinting experiments (McBryant *et al.*, 1995).

that if a specific α helix was most involved in WT1 Pel22 binding, its replacement with the corresponding sequence from an α-helix of finger 4, 5, 6 or 7 from TFIIIA would result in loss of specificity for the WT1 ligand Pel22 RNA. By comparing dissociation constants of mutant WT1 proteins to wild type WT1, we expected to identify which zinc finger α helix was most critical for RNA interactions.

3.1.5. Mutant construction by two different methods of site-directed mutagenesis

To determine which zinc finger or fingers were most important for WT1 interaction with RNA, four mutants were constructed using site-directed mutagenic PCR. Each mutant construct had the α helical region of one zinc finger altered by replacing it with a corresponding α helix from zinc fingers 4-7 of TFIIIA (Figure 8).

The clones Wx1B+ and Wx2B+ were given to me by Dr. Romaniuk cloned into pCRT7/NT-TOPO (Invitrogen). Wx4B+ was given to me as a purified PCR product, and the mutagenic PCR of Wx3B+ was completed by myself.

3.1.6. Diagnostic tests

Examples from diagnostic tests that were used in the development of the α helix swap mutants of WT1 will be shown and discussed.

3.1.6.1. Diagnostic Restriction Enzyme digests

In order to screen clones for plasmids that contained the correct insert, diagnostic restriction enzyme digests were employed that utilized unique restriction enzyme sites that are not present in the WT1 wild type sequence. Isolated pET100/D-TOPO plasmids that potentially contained the Wx1B+ insert were digested with the enzyme PvuII, with plasmids containing the mutant insert predicted to produce bands

of 2750bp, 1653 bp, 1502bp, 227bp, 94bp, and 93bp. The potential Wx2B+-pET100/D-TOPO plasmids were similarly digested with the enzyme AflII which is predicted to linearize the plasmid with a corresponding band size of 5741 bp. All plasmids that exhibited the correct banding pattern for the diagnostic restriction enzyme digest were further screened by PCR. Figure 12 shows the results of the Wx2B+ AflII digest, with plasmids in lanes 5,7, and 11 producing products of the correct size.

3.1.6.2. Diagnostic PCR

The Wx1B+ and Wx2B+ plasmid clones that passed the restriction enzyme test were further screened by PCR. Oligonucleotides were used that prime just up and down stream of the ET100/D-TOPO multiple cloning site, and PCR products were analyzed on a 1% agarose gel with an expected product size 811 (Figure 13). Clones that passed both the restriction enzyme and PCR diagnostic tests were sequenced at the CBR sequencing facility. Only clones that had the correct sequence for each mutant were used in protein purification and expression.

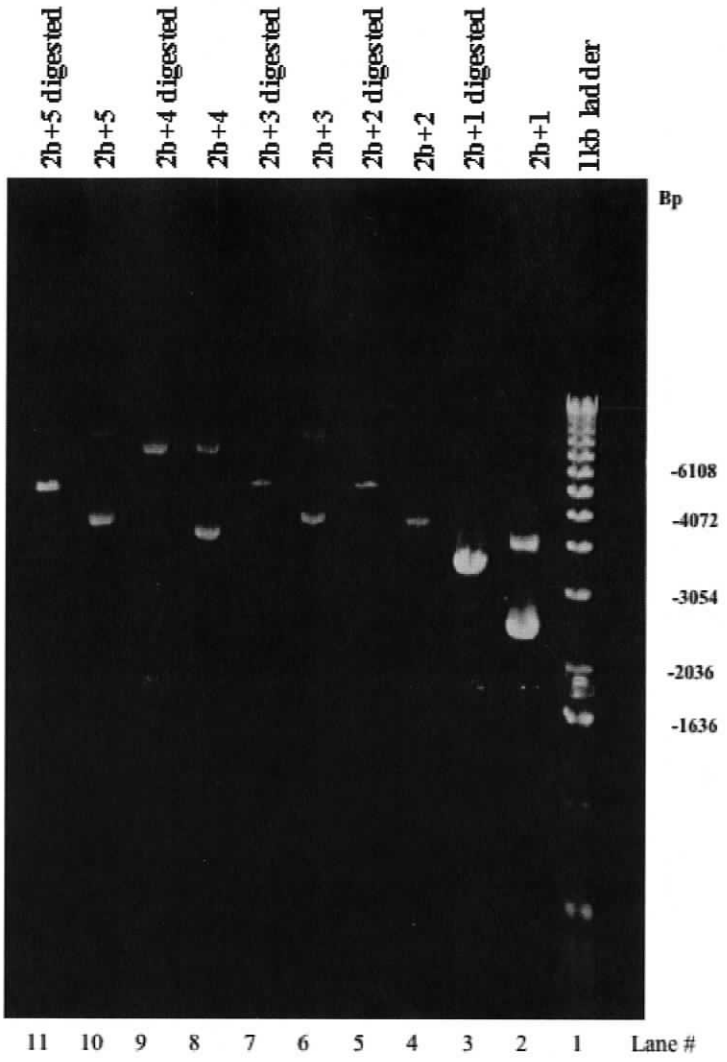

Figure 12. 0.8% agarose gel showing restriction fragment screening of potential pET30 plasmids for those containing the Wx2B+ insert. Expected product of AflII digest if the correct insert is present is a linear band of 5741bp. Clones 2, 3, and 5 in lanes 5, 7 and 11 exhibit the correct banding pattern.

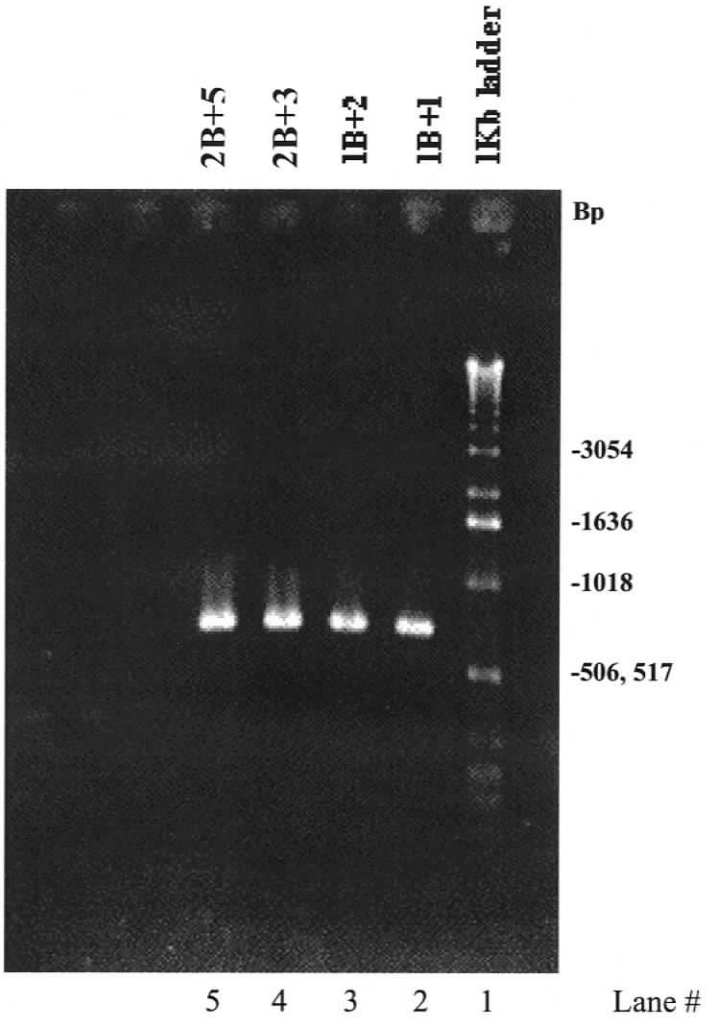

Figure 13. Results of the diagnostic PCR of Wx1B+ and Wx2B+ potential clones analyzed on a 1.0% agarose gel. Plasmid containing the correct size insert were expected to produce a band of 818bp. All clones on this gel exhibit an insert of the correct size.

3.1.6.3. Colony PCR

The Wx3B+ and Wx4B+ mutants were screened by a slightly different method than the Wx1B+ and Wx2B+ clones. After ligation of PCR products into pET30a, the ligation reaction was transformed into *E. coli* DH5α cells and plated out to yield individual colonies. At this point colony PCR was used as the initial diagnostic test to indicate which colonies contained products of the correct size. Figure 14 shows the results of the PCR reaction. Colonies that showed an insert of the correct size were grown up and plasmids were isolated for further screening.

3.1.7. Protein purification

The plasmids containing the mutant clones (TFIIIA swap mutants, p43 swap mutants and WT1 deletion mutants) and wild type proteins were used to transfect either BL21 (DE3) or BL21(DE3) plysS expression strains of *E. coli*. Protein was expressed at high levels by the presence of the T7*lac* promoter in the plasmids used which has been modified to contain a *lac* operator sequence. T7 RNA polymerase was provided by the BL21 (DE3) or BL21 (DE3) pLysS strains of *E. coli* that contain a *lac* construct that encodes for T7 RNA polymerase under the control of the *lac*UV5 promoter which can be de-repressed by IPTG. Proteins were purified using NT-Nickel columns which have HIS tag affinity. Protein purity and size was confirmed by running the purified protein fractions on 15% SDS-page gels and staining with coomassie blue. The mutants and wild type WT1 generally ran with an apparent size of 27kDa (Figure 15), while the actual predicted size of the protein based on amino

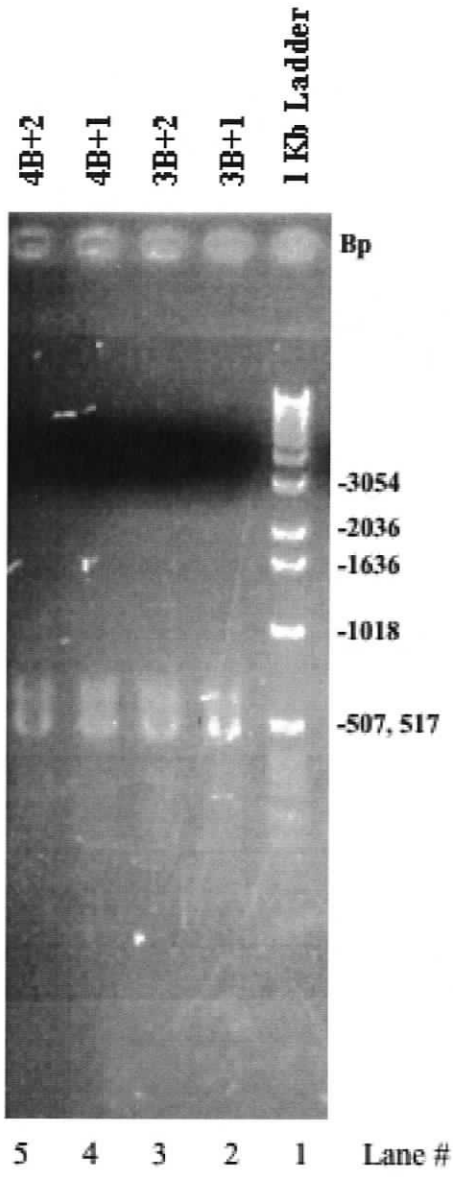

Figure 14. An example of a 1.0% agarose gel of PCR products from colony PCR of colonies containing pET30a plasmids with potential Wx3B+ and Wx4B+ inserts. The expected insert size of a positive clone is 463bp, and all of the clones on this gel show the correct size insert.

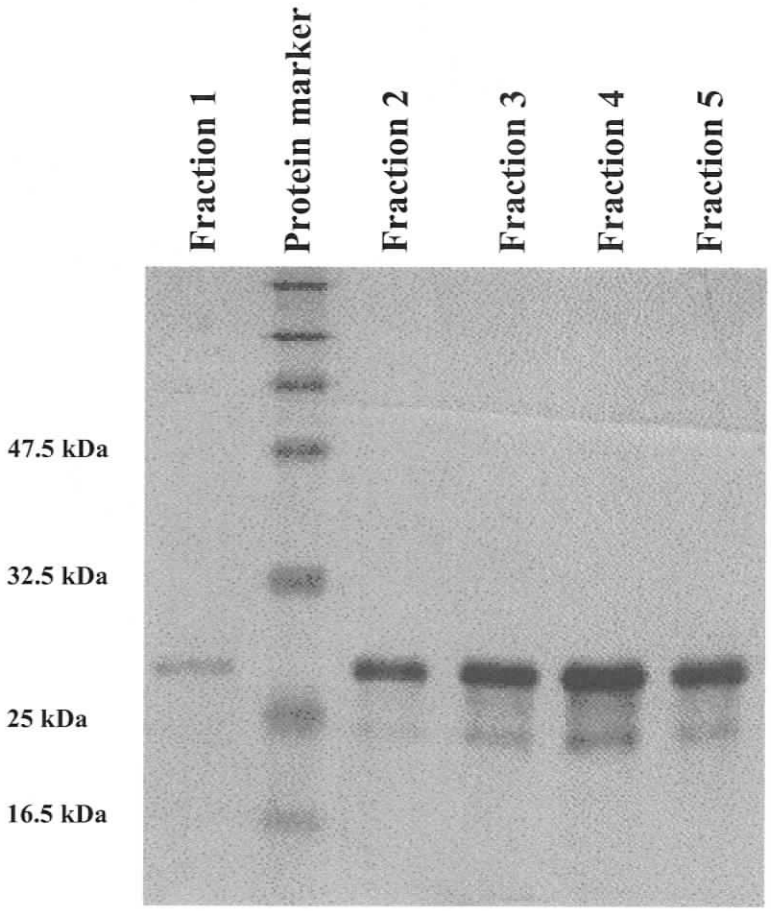

Figure 15. An example of purified WT1(KTS)ZF protein fractions ran on a 15% SDS-PAGE gel and stained with coomassie blue. WT1(KTS)ZF runs with an apparent weight of approximately 27kDa.

acid content is 22kDa. A possible reason for this discrepancy is that WT1 contains many basic residues which cause it to migrate slower under SDS-page conditions. The concentration of the proteins were determined by the Bradford method using Bradford Reagent (Bio-Rad) with Bovine Serum Albumin as the standard. Protein concentrations for the mutant and wild type proteins ranged from 17μM to 300μM.

3.1.8. Filter binding assays

3.1.8.1. Quantitative binding of Wx+ mutants with the RNA aptamer Pel22

The equilibrium binding of the Wx+ mutants to the RNA aptamer Pel22 were measured using a nitrocellulose binding assay (Romaniuk, 1985; Romaniuk, 1990) and the binding curves from three or more independent experiments are shown in Figure 16. Wild type WT1(KTS)ZF binds to a consensus binding region within the Pel22 sequence (Figure 17). In order to determine if the mutations made within the α helical regions of WT1(KTS)ZF resulted in a decrease in affinity for Pel22, the binding dissociation constants of each Wx+ mutant for Pel22 RNA were determined by the nitrocellulose filter binding assay and compared to the K_d determined for wild type WT1(KTS)ZF for Pel22 (Table 6). The results of three or more independent experiments indicate that WT1(KTS)ZF binds to Pel22 with a K_d of 86 ± 18.0 nm and that all four of the mutants bind to Pel22 with similar affinities, with K_d values that are less than 2 orders of

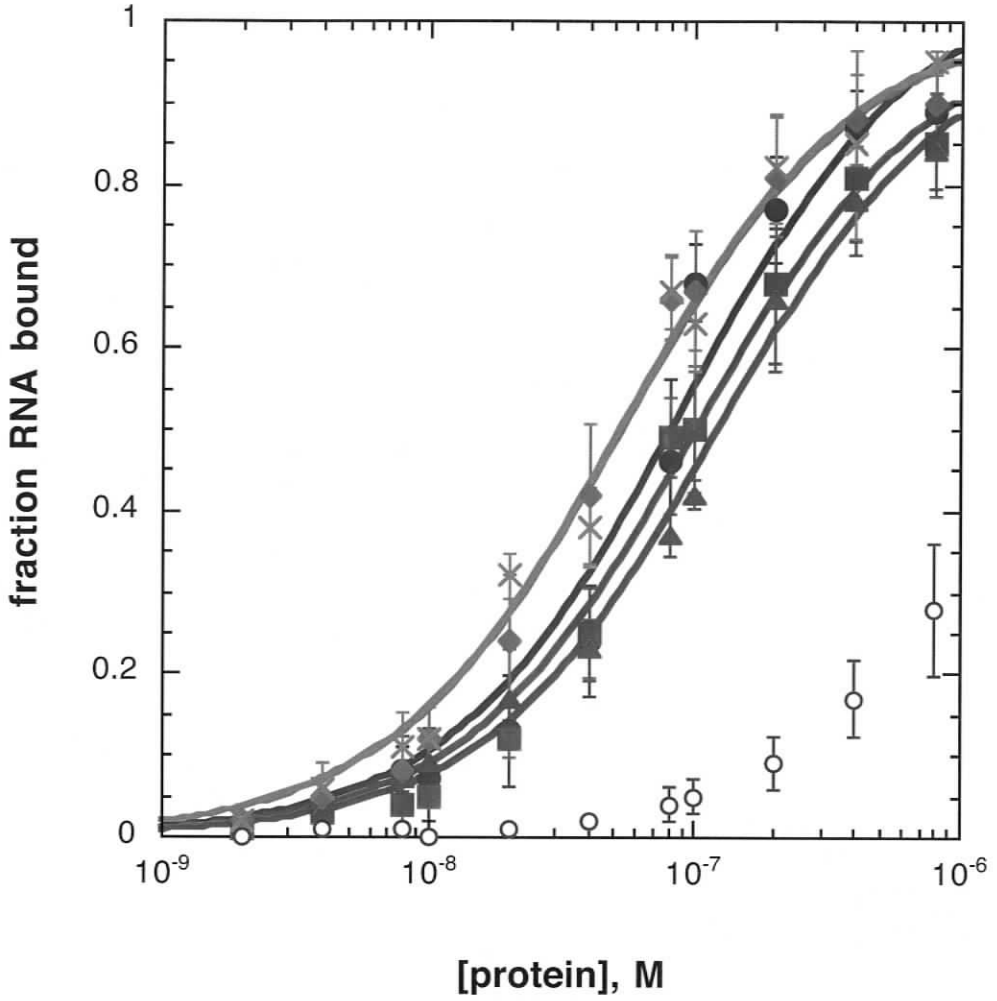

Figure 16. Equilibrium binding of wild type WT1(KTS)ZF (●) and the mutants Wx1B+ (■), Wx2B+ (▲), Wx3B+ (◆) and Wx4B+ (×) with Pel22 RNA. The equilibrium binding of wild type with 5S RNA (○) was used as a negative control for non-specific interactions and was not fit to the bimolecular equilibrium equation because binding affinity was too low to determine accurately.The binding curves shown are the average of 3 or more independent experiments and error bars represent the standard deviation of fraction RNA bound at each protein concentration.

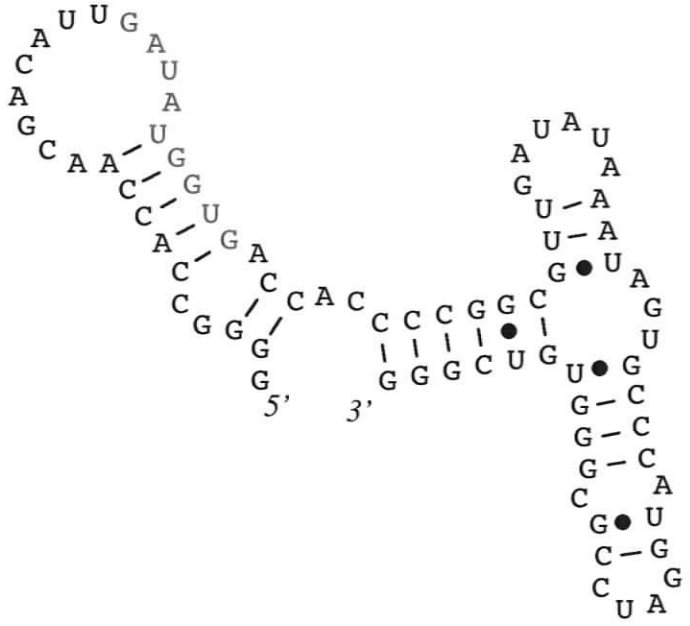

GGGGCCACCAACGACAUUGAUAUGGUGACCACCCCGGCGUUGAUAUAA
AUAGUGCCCAUGGAUCCGCGGGUGUCGGG

Figure 17. Top. Lowest-free energy structures predicted Pel22, as determined by the mfold program (Zhai *et al.*, 2001). Bottom. The sequence of Pel22 RNA (Bardeesy and Pelletier, 1998). The consensus sequence is shown in red.

Table 6. Dissociation constants of wild type and mutant WT1 peptides for Pel22 and 5S RNA calculated from the average of three or more equilibrium binding assays fitted to the bimolecular equilibrium equation. The relative affinities were determined by dividing the K_d of wild type WT1 for Pel22 by the K_d of the mutant for Pel22. The relative specificity was determined by dividing the K_d of the protein for 5S RNA by the K_d for Pel22 RNA. *The binding affinity was too low to be determined accurately, and data could not be fit accurately to the bimolecular equilibrium equation.

Protein	Pel22 K_d (nM)	5S K_d (nM)	Relative Affinity	Relative Specificity
Wild type	86 ± 18.0	>1000*	1.0	≥ 12
Wx1B+	102 ± 11.0	>1000*	0.83 ± 0.17	≥ 12
Wx2B+	123 ± 11.0	>1000*	0.50 ± 0.12	≥ 12
Wx3B+	54 ± 5.8	279 ± 70	1.78 ± 0.47	5.1 ± 1.2
Wx4B+	53 ± 6.4	68 + 24	1.68 ± 0.19	1.3 ± 0.46

magnitude higher or lower than wild type. The mutants Wx1B+ and Wx2B+ bind to Pel22 with slightly less affinity than wild type with K_d values of 102nm ± 11.0nm and 123nm ± 11.0nm respectively, while the mutants Wx3B+ and Wx4B+ bind to Pel22 slightly better than wild type with K_d values of 54 ± 5.8 and 53 ± 6.4. The relative affinities of each mutant were compared (Table 6), and the largest change in affinity compared with wild type was seen by the mutant Wx3B+ (1.78 ± 0.47).

3.1.8.2. Quantitative filter binding of the Wx+ mutants with 5S RNA

In order to examine the binding properties of the Wx mutants in another manner, equilibrium binding of the mutants with 5S RNA were carried out to see if any of the mutants exhibited a change in ligand specificity. The mutant that demonstrated the largest difference in 5S binding was Wx4B+ (Figure 18). Wild type WT1(KTS)ZF does not bind to 5S RNA and the K_d cannot be determined accurately and is described as being greater that 1000 nm. As Table 6 demonstrates, the mutants Wx3B+ and Wx4B+ acquire the ability to bind to 5S RNA. The mutant Wx4B+ demonstrates this most dramatically with a specificity ratio that is at least 10X smaller than wild type (a specificity ratio of 1.2 ± 0.46 compared with the specific ration of ≥12 for wild type WT1.

3.1.8.3. Qualitative filter binding of the donor peptide TFIIIA4-7

There are two possible reasons why none of the mutants that were constructed resulted in ablation of Pel22 binding. The first possibility is that our initial hypothesis was incorrect, and WT1 does not bind to RNA through interaction of the α helices as

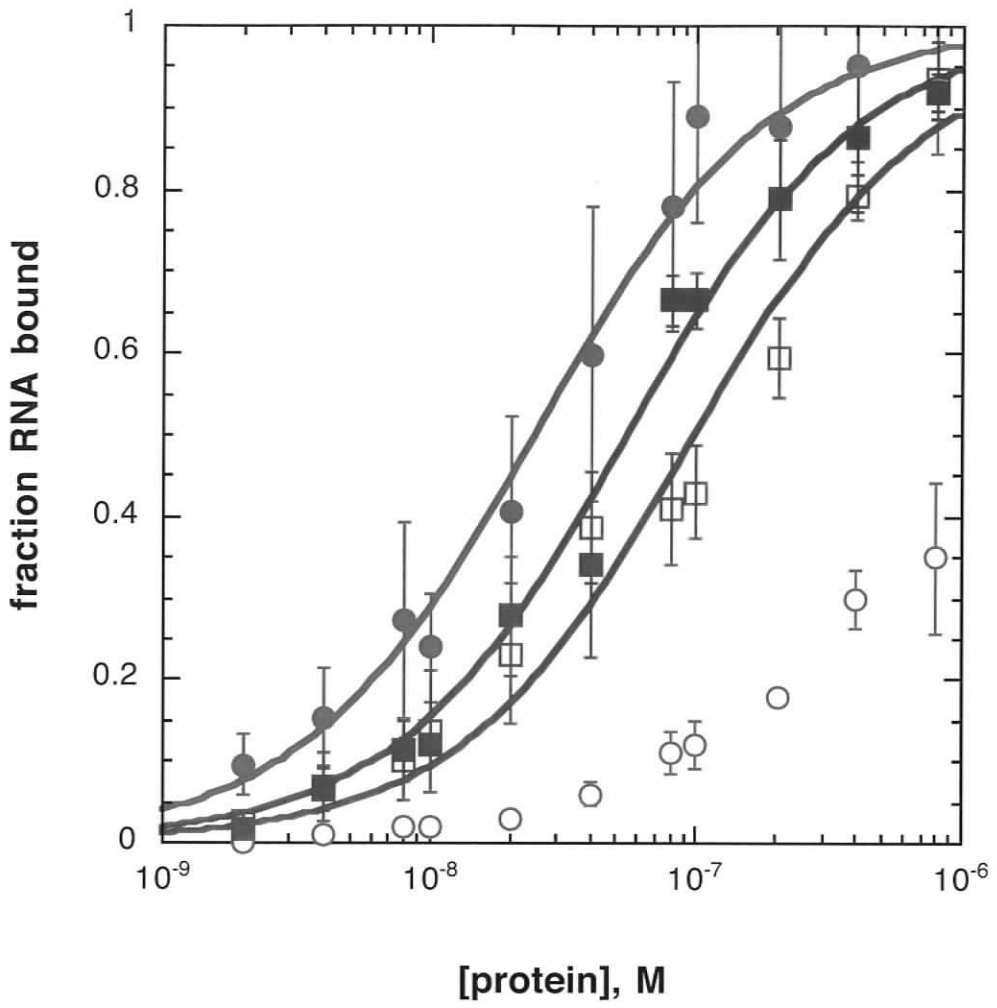

Figure 18. Equilibrium binding of wild type WT1(KTS)ZF with Pel22 (●) and 5S RNA (○) compared to that of the mutant Wx4B+ with Pel22 (■) and 5S RNA (□). The equilibrium binding of wild type with 5S RNA (○) was not fit to the bimolecular equilibrium equation because binding affinity was too low to determine accurately. The binding curves shown are the average of 3 or more independent experiments and error bars represent the standard deviation of fraction RNA bound at each protein concentration.

other zinc finger proteins do. The other reason may be that the zinc finger peptide of fingers 4-7 of TFIIIA may actually bind to Pel22. This phenomenon would be unexpected, considering that full length TFIIIA does not bind to Pel22, but it was the easiest possibility to test. Equilibrium binding of TFIIIA4-7 was probed with 5S RNA and Pel22 RNA (Figure 19) in both 1 mM and 5 mM $MgCl_2$ because the bindings with WT1 and the mutants were all done in 1 mM $MgCl_2$, whereas past experiments with full length TFIIIA and RNA (Hamilton *et al.*, 2001) was done in 5 mM $MgCl_2$ (Figure 10). At a $MgCl_2$ concentration of 1 mM, TFIIIA4-7 bind to both 5S RNA and Pel22 RNA with K_d values of 149 nm and 191nm respectively, while at 5mM it binds to 5S RNA and Pel22 with K_d values of 1.7 nm and 152 nm respectively. The finding that TFIIIA4-7 binds to both 5SRNA and Pel22 with similar affinities at 1 mM $MgCl_2$ indicates that this peptide was not the best choice for creating zinc finger mutants to probe WT1 binding specificity.

3.2. p43 swap and WT1 deletion mutants to further probe WT1 RNA binding

3.2.1. Overview

The experiments using the TFIIIA4-7 swap mutants were not informative because of the unexpected result that the peptide TFIIIA4-7 itself binds to Pel22. It would be unexpected to see a decrease in Pel22 specificity in a mutant that was created by swapping zinc fingers with another peptide that also bound to the same ligand. In order to make swap mutants that will be able to give us insight into the mode of WT1 RNA recognition, a donor peptide must be used that follows two parameters. A) It does not bind to Pel22 so that if an important finger is replaced, a decrease in affinity for Pel22

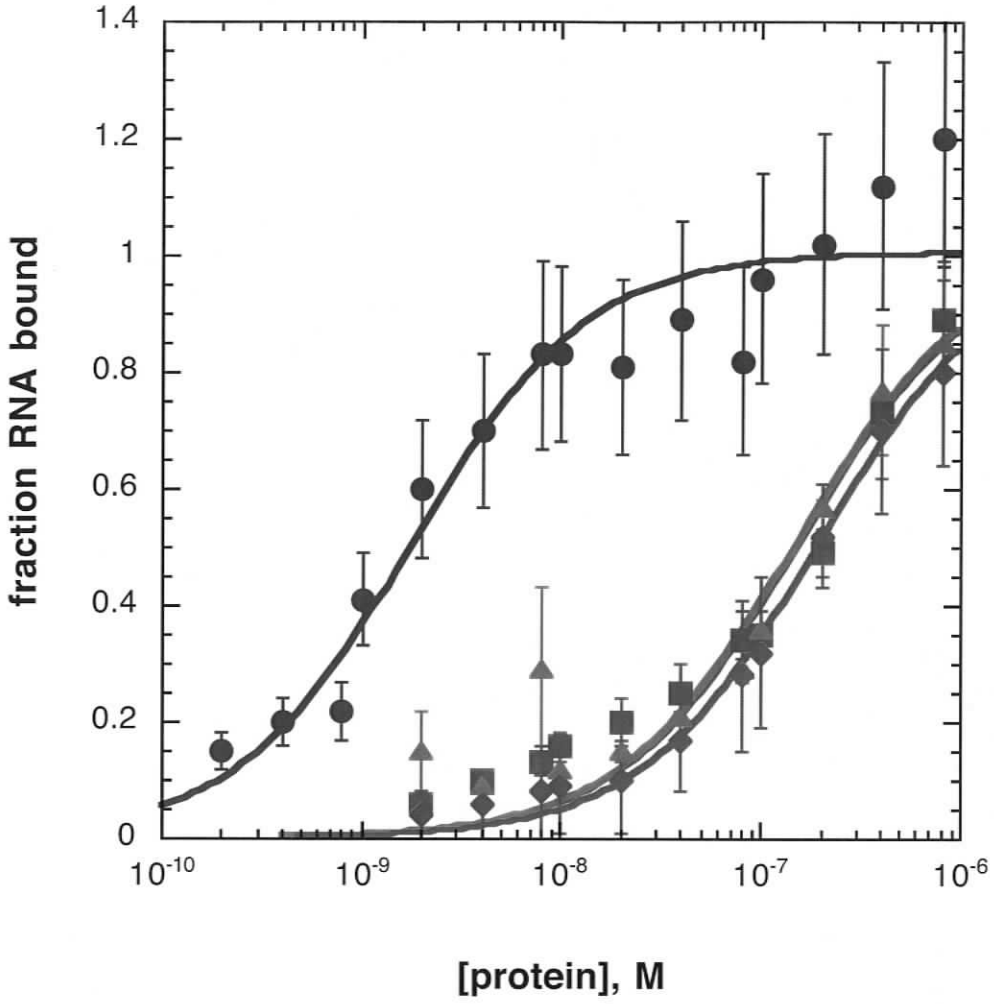

Figure 19. Equilibrium binding at 1 mM $MgCl_2$ concentration of the peptide TFIIIA 4-7 with Pel22 (▲) and 5S RNA (■) and equilibrium binding at 5 mM $MgCl_2$ concentration with Pel22 (◆) and 5S RNA (●). The binding curves shown are the average of 3 or more independent experiments and error bars represent the standard deviation of fraction RNA bound at each protein concentration.

can be observed and B) it preferably does not bind to 5S RNA so that we can use 5S RNA again as a negative control for non-specific RNA interactions.

3.2.2. p43: another *Xenopus* zinc finger protein that binds to 5S RNA

The *Xenopus* 9 zinc finger protein interacts with 5S RNA within the 42 S RNP particle (Denis and Mairy, 1972). The interaction of p43 with 5S RNA has been previously characterized by our laboratory (Zang and Romaniuk, 1995; Zang *et al.*, 1995; Hamilton *et al.*, 2001).

The mechanism by which p43 binds to 5S RNA is currently being examined by our laboratory. For that study, two recombinant peptides of p43 were constructed, the first containing the four zinc fingers 1 through 4, and the second containing the zinc fingers 6 through 9. Because these two peptides were readily available and already expressed and purified (by Dr. Romaniuk and Tristen Weiss), binding experiments were done to see if either of them would fit the parameters indicative of a good WT1 swap donor (does not bind to Pel22 or 5S RNA).

3.2.3. p43 6-9: the perfect WT1 swap donor peptide

The equilibrium binding of the p43 peptides p43 1-4 and p43 6-9 to Pel22 RNA and 5S RNA was assessed in order to find a new donor peptide for construction of WT1 zinc finger mutants (Figure 20). In order to be a good donor, the peptide in question must have low affinity for Pel22 RNA and in an ideal scenario would also have low, if any, affinity for 5S RNA. As Figure 20 demonstrates, p43 6-9 fits both of these parameters and did not have affinity for either of the RNA ligands.

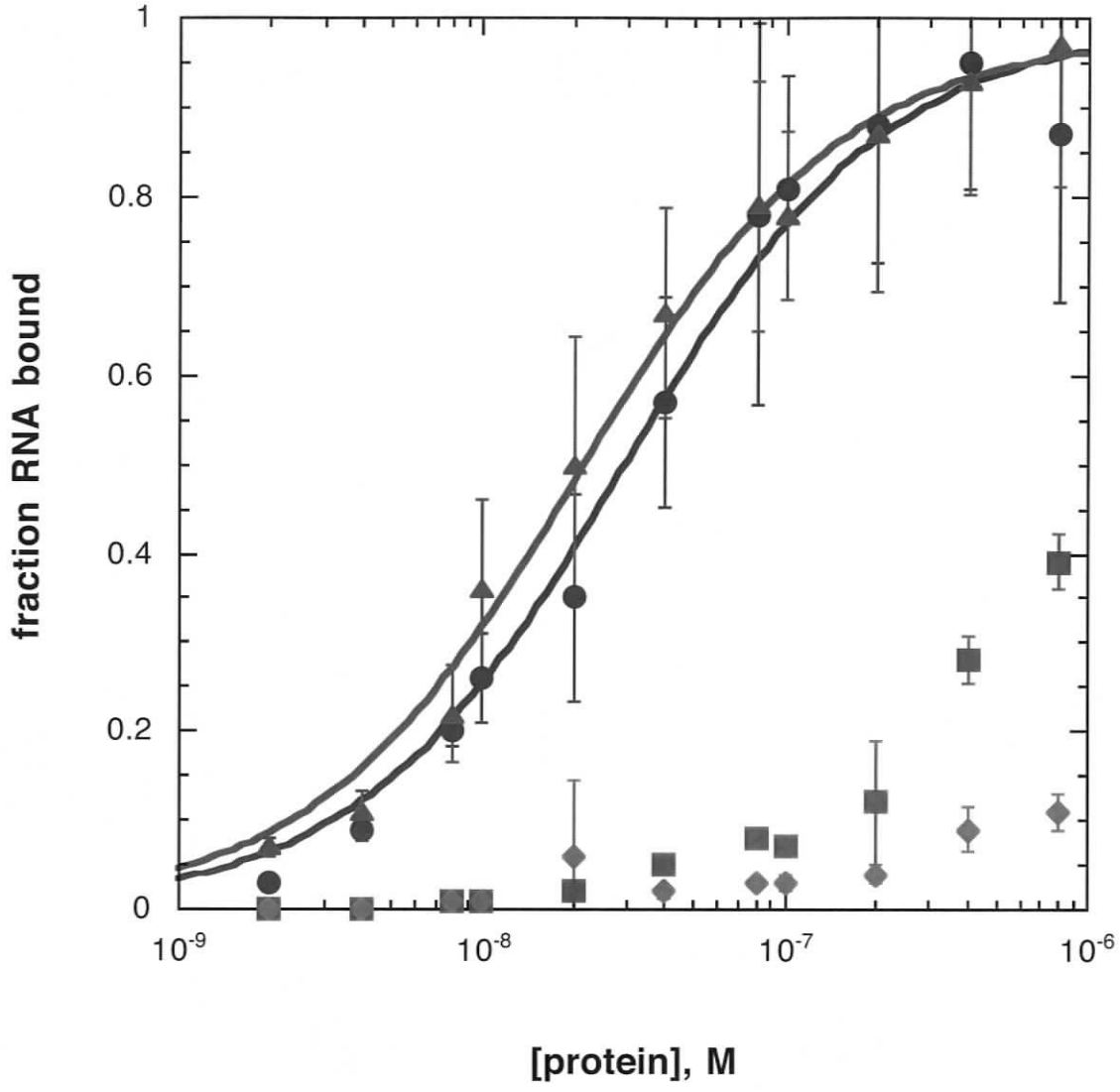

Figure 20. Equilibrium binding of the peptide p43 1-4 with Pel22 (●) and 5S (▲) and the peptide p43 6-9 with Pel22 (■) and 5S RNA (◆). The equilibrium binding of p43 6-9 with Pel22 (■) and 5S RNA (◆) was not fit to the bimolecular equilibrium equation because binding affinity was too low to determine accurately. The binding curves shown are the average of 3 or more independent experiments and error bars represent the standard deviation of fraction RNA bound at each protein concentration.

In order to try and probe the RNA interaction of WT1, more swap mutants were constructed this time using the cDNA of fingers 6-9 of p43 as the donor sequence. The first set of mutants consisted of 4 complete fingers swaps in comparison with the Wx mutant swaps where only the α helix was replaced. The Wx mutants were constructed under the assumption that WT1 interacts with RNA in a similar manner as TFIIIA (through the α helix) but it was thought that this might not necessarily be the case with WT1 and replacing entire zinc fingers will ensure that we control for this possibility. The first set of 4 mutants that were created are depicted in Figure 8. Wp1 has finger 1 of WT1 replaced with finger 6 of p43, Wp1-2 has fingers 1 and 2 of WT1 replaced with fingers 6 and 7 of p43, Wp3-4 has fingers 3 and 4 of p43 replaced with fingers 8 and 9 of p43 and Wp4 has finger 4 replaced with finger 9 of p43. It was hoped that by making larger substitutions it would be possible to determine which region of WT1 is most crucial in the RNA interaction, and then make smaller substitutions to determine which individual zinc finger is most important.

3.2.4. Equilibrium binding of p43 swap mutants

The affinity of each p43 finger swap mutant for Pel22 was assessed by equilibrium binding (Figure 21), with the binding of p43 6-9 to Pel22 used as an internal assay control to ensure that there is no non-specific binding occurring.

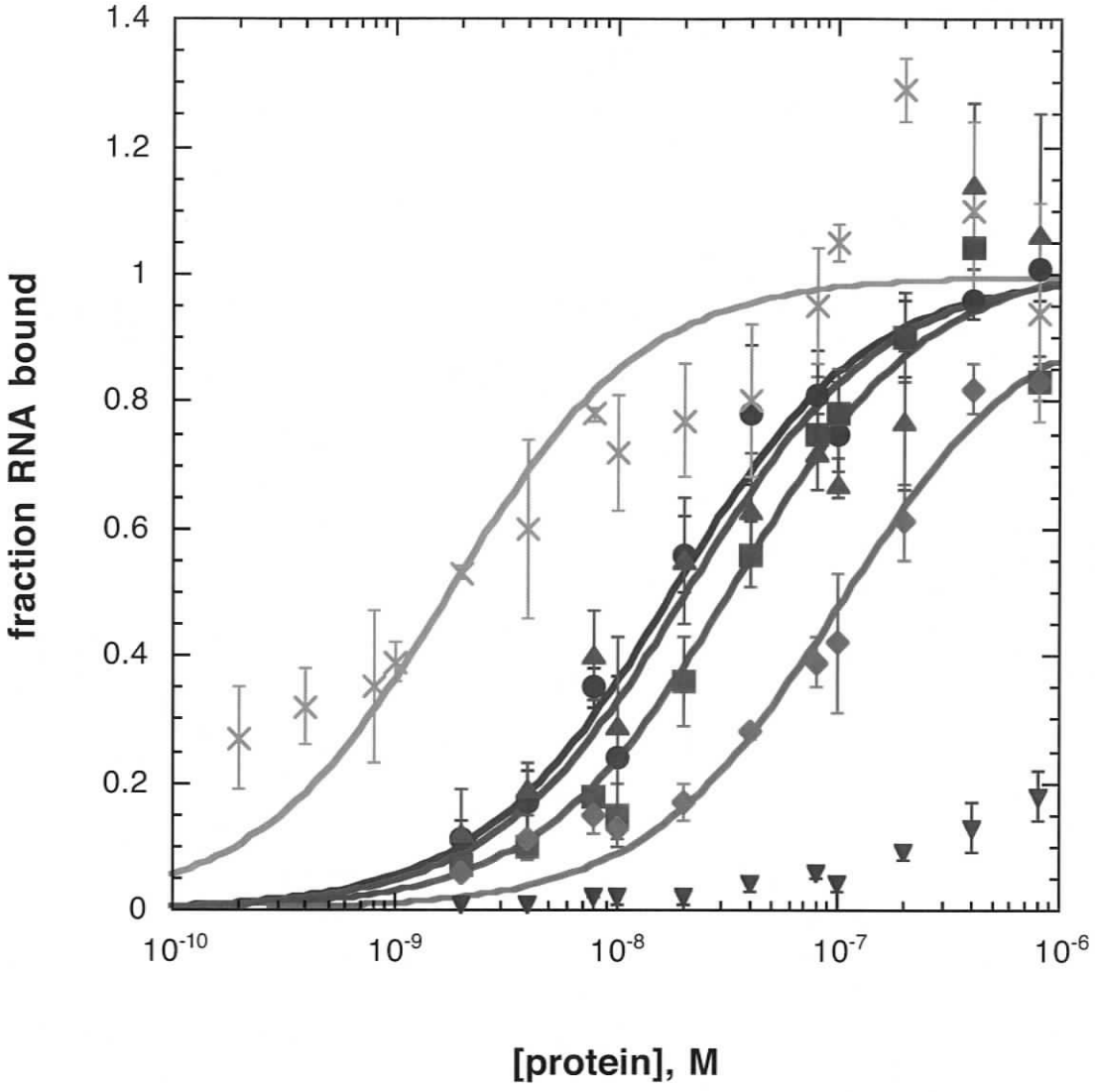

Figure 21. Equilibrium binding of wild type WT1(KTS)ZF (●) and the mutants Wp1 (■), Wp1-2 (▲), Wp3-4 (◆) and Wp4 (×) with Pel22 RNA. The equilibrium binding of p43 6-9 with Pel22 RNA (▼) was used as a negative control for non-specific interactions and was not fit to the bimolecular equilibrium equation because the binding affinity was too low to determine accurately. The binding curves shown are the average of 3 or more independent experiments and error bars represent the standard deviation of fraction RNA bound at each protein concentration.

data in Table 7 shows, the mutant with Finger 1 replaced (Wp1) and the mutant with both finger 1 and 2 replaced (Wp1-2) bind to Pel22 RNA with roughly the same affinity as wild type WT1, with the finger 1 replacement showing a modest 2 fold decrease in affinity. The most dramatic decrease in affinity for Pel22 RNA was demonstrated by replacement of fingers 3 and 4, which bound to Pel22 roughly 6X less than wild type with a relative affinity of 0.17 ± 0.02. Surprisingly, the mutant that had finger 4 of WT1 replaced (Wp4), showed a dramatic increase in affinity for Pel22 RNA, and bound to the Pel22 RNA ligand 10 times better than wild type with a relative affinity of 10.11 ± 2.9.

The finding that Wp4 could bind readily to Pel22 with a 10X higher affinity than wild type, and the finding that Wp3-4 bound to Pel22 with a 6X decrease in affinity has important implications. The only difference between these two mutants, is the replacement of finger three of WT1. If we compare equilibrium binding of Wp3-4 with Wp4 alone, we see a 60-fold difference between these two mutants, which must be mediated through the interaction of RNA with finger 3 of WT1.

3.2.5. Equilibrium binding of WT1 deletion mutants

Previous literature on the nature of WT1 RNA binding contains contradictions concerning which WT1 zinc finger is absolutely crucial for RNA binding. Some studies have shown that when finger four is deleted this results in ablation of RNA binding affinity (Bardeesy and Pelletier, 1998), while another study has shown the same result for finger 1 deletion mutants (Caricasole *et al.*, 1996). In order to investigate the binding properties of these two WT1 mutants in a quantitative manner, equilibrium binding experiments were used to assess each mutant's affinity for Pel22

Table 7. Relative affinities and relative specificities of the p43-swap and WT1 deletion mutants in comparison to wild type WT1 –KTS ZF. The relative affinities were determined by dividing the K_d wild type WT1 for Pel22 by the K_d the mutant for Pel22. The relative specificity was determined by dividing the K_d of the protein for 5S RNA by the K_d of the protein for Pel22 RNA. *The binding affinity was too low to be determined accurately.s

Protein	Pel22 K_d (nM)	5S K_d (nM)	Relative Affinity	Relative Specificity
Wild type	18.2 ± 2.9	≥1000*	1.0	≥ 50
Wp1	34.2 ± 6.4	≥1000*	0.48 ± 0.08	≥ 50
Wp1-2	21.1 ± 6.3	≥1000*	0.85 ± 0.2	≥ 50
Wp3-4	103 ± 19	≥1000*	0.17 ± 0.02	6.8 ± 0.51
Wp4	1.5 ± 0.9	1.9	10.11 ± 2.9	1.27 ± 0.5
W12P8W4	139 ± 8.2	≥1000*	≤ 0.13 ± 0.01	≤ 7.2
WT1ΔF1	16 ± 2.08	≥1000*	1.11 ± 0.17	≥ 50
WT1ΔF4	≥1000*	≥1000*	≤ 0.01 ± 0.0*	≤ 0.01 ± 0*

RNA in comparison to wild type affinity (Figure 22). The results from these experiments are very clear. As can been seen in Table 4, the WT1 mutant lacking finger 4 (WT1Δ4) shows no specificity for Pel22 RNA with a relative affinity of 0.01 ± 0.0 compared to wild type. Comparatively, the mutant that has finger 1 of WT1 replaced had virtually the same affinity for Pel22 as wild type WT1 with a relative affinity value of 1.1 ± 0.17.

3.2.6. Equilibrium binding by W12P8W4

The results from the above experiments prompted us to construct a mutant that had only finger 3 of WT1 replaced with finger 8 of p43 (W12P8W4). This mutant was assessed for Pel22 binding affinity by filter binding, and the equilibrium dissociation constant was determined (Figure 23). Results from these experiments are not as clear as would be expected. The binding curve of the mutant did not completely reach the plateau of the curve within the protein range used. However, an experiment was done at a higher protein concentration for both wild type and the mutant (not shown), wild type affinity for Pel22 was reduced for reasons that remain unclear (assumptions that must be met to use the assay have not been tested under conditions required for proper folding of zinc fingers at higher protein concentrations). From the data that was obtained from experiments in the 1 to 800 nm protein concentration range (Table 7), it can be deduced that the mutant W12P8W4 has at least a 5 to 10 fold reduction in affinity for Pel22 in comparison to wild type WT1. It is possible that the reduction in affinity is much greater; however, due to limitations with the assay, it is not possible to determine this at the present time.

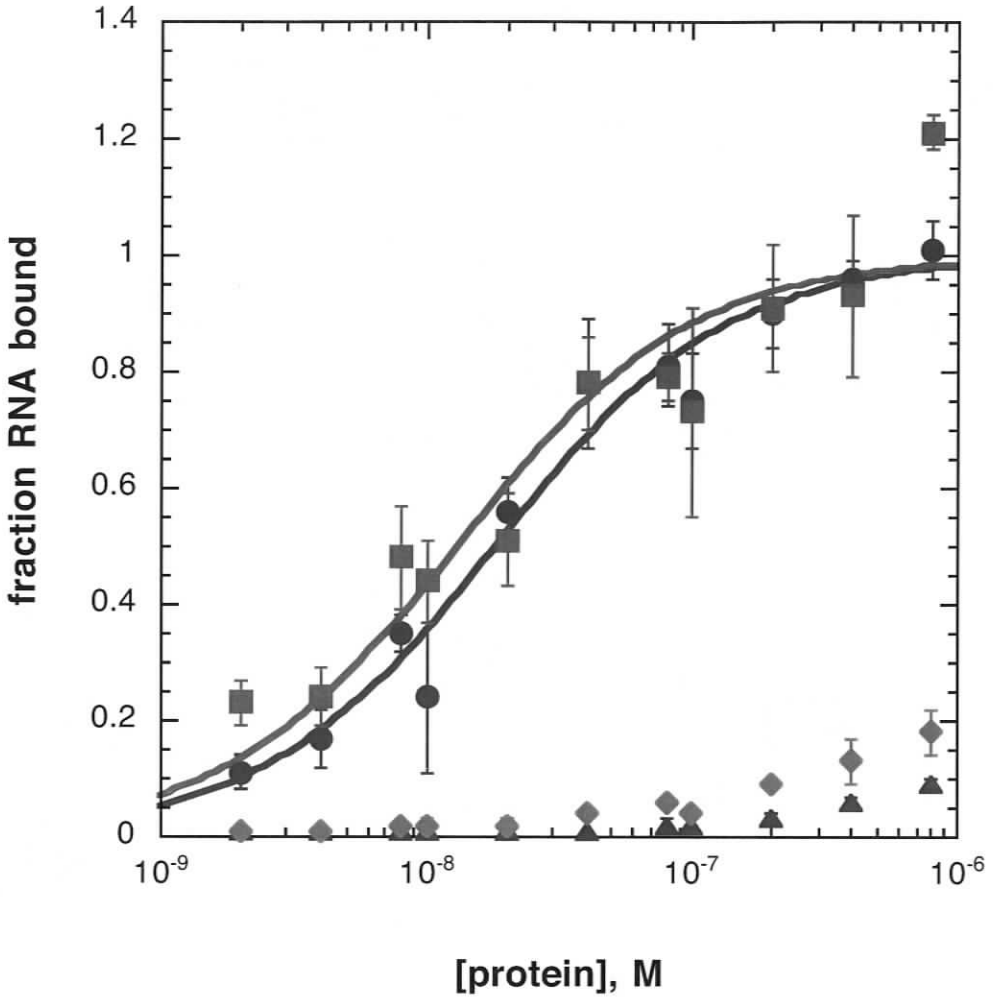

Figure 22. Equilibrium binding of wild type WT1 –KTS ZF with Pel22 (●) and the deletions mutants WT1ΔF1 with Pel22 (■) and WT1ΔF4 with Pel22 (◆). The equilibrium binding of p43 6-9 with Pel22 (▲) was used as a negative control for non-specific RNA interactions and p43 6-9 and Wp4 Pel22 data were not fit to the bimolecular equilibrium equation because binding was too low to determine accurately. The binding curves shown are the average of 3 or more independent experiments and error bars represent the standard deviation of fraction RNA bound at each protein concentration.

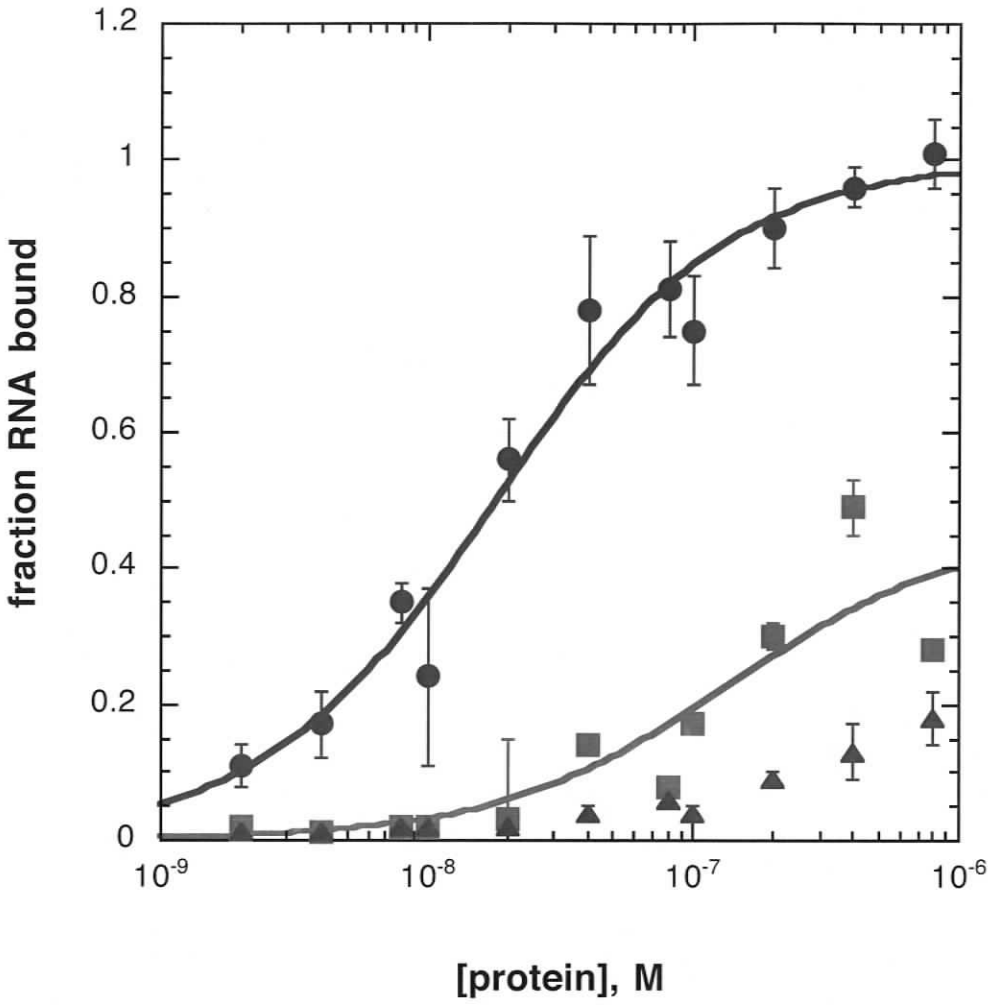

Figure 23. Equilibrium binding of the mutant W12P8W4 with Pel22 (●) and 5S (■) RNA. p43 binding with Pel22 (▲) was used as a negative control for non-specific RNA interactions and was not fit to the bimolecular equilibrium equation because binding affinity was too low to determine accurately. The binding curves shown are the average of 3 or more independent experiments and error bars represent the standard deviation of fraction RNA bound at each protein concentration.

3.2.7. Specificity of the p43 swap mutants and WT1 deletion mutants

Unlike the Wx mutants, which were swapped with a peptide that had affinity for 5S RNA itself, the Wp mutants were constructed using the cDNA from the p43 6-9 peptide that does not bind to 5S RNA. Because wild type WT1 binds to 5S RNA with very low affinity, it is possible to determine the specificity ratio for each WT1 mutant. Equilibrium binding assays were used to determine the affinity of each mutant for 5S RNA in comparison to Pel22 RNA. The K_d values determined by equilibrium binding with 5S RNA was divided by the K_d values determined for Pel22 to give a specificity ratio (Table 7). The mutants Wp4, Wp3-4 and W12P8W4 demonstrated a decreased RNA binding specificity to wild type WT1; however, only the mutant Wp4 was able to bind to 5S RNA with a dramatically higher affinity than wild type WT1 (Figure 24). This mutant had a specificity ratio for Pel22 that was 43 times less than wild type.

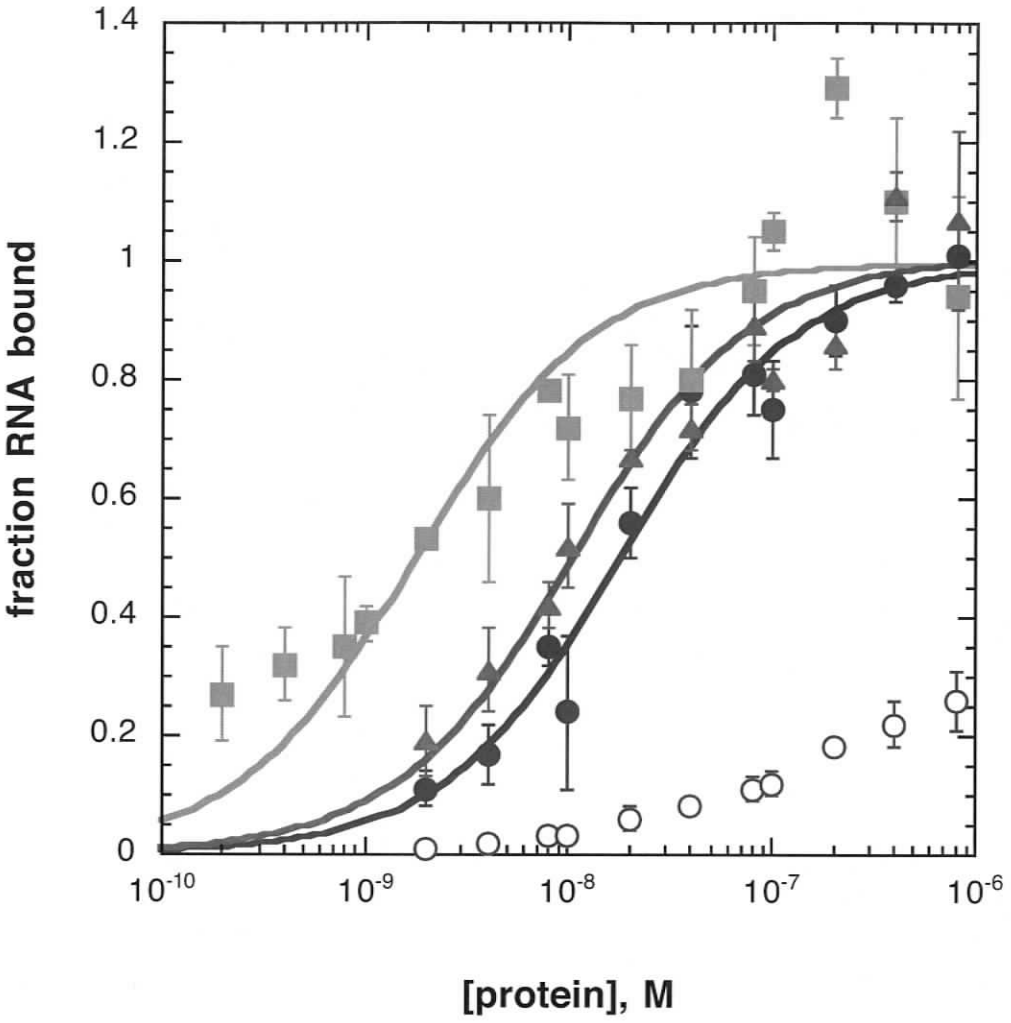

Figure 24. Equilibrium binding of wild type WT1 –KTS ZF with Pel22 (●) and 5S RNA (○) compared to that of the mutant Wp4 with Pel22 (■) and 5S RNA (▲). The binding curves shown are the average of 3 or more independent experiments and error bars represent the standard deviation of fraction RNA bound at each protein concentration.

Chapter 4. Discussion

mRNA plays a vital role in cellular processes, and the mechanisms of mRNA splicing, editing, localization, export and stability are important to understand since there is increasing evidence linking defects in mRNA metabolism with human disease. Studies on mRNA metabolism and function will not only increase our understanding of the cause and progression of disease, but also will provide a powerful tool with endless possible entry points for therapeutic intervention. One of the largest groups of proteins that are known to be involved in gene expression and regulation are zinc finger proteins (Krishna *et al.*, 2003). Zinc finger proteins are particularly interesting, as numerous reports have identified proteins within this class of molecules that exhibit multi-functionality (Laity *et al.*, 2001). Many zinc finger proteins bind not only to DNA, but also have the ability to bind to RNA and can mediate protein-protein interactions (Iuchi, 2001; Hall, 2005). This diverse range of functions implicates zinc finger proteins as complex regulators of gene networks and implicates their potential involvement in disease on many different biochemical levels.

This study has concentrated on the zinc finger protein WT1. The primary transcript of WT1 undergoes two pre-mRNA splicing events (Haber *et al.*, 1991) to produce four main isoform products. The first alternative splice is encoded by exon 5, and introduces 17 amino acids between the proline-glutamine rich transactivation domain of the N-terminus and the zinc finger domain of the C-terminus. The second alternative splice is encoded by exon 9 and introduces the amino acids KTS between

fingers 3 and four of the zinc finger domain. The –KTS and +KTS isoforms of WT1 are particularly interesting because they appear to have different functional roles within the cell. –KTS seems to function as a typical transcription factor, and modulates the expression of a variety of genes including amphiregulin, Bcl-2, and Wnt (Lee and Haber, 2001). The function of +KTS on the other hand can only be speculated on. The insertion of KTS in between zinc fingers 3 and 4 disrupts the DNA binding activity of the protein suggesting that this isoform is not directly involved in transcriptional regulation. However, the +KTS isoform has been found to preferentially localize to areas of the cell associated with RNA processing (Charlieu *et al.*, 1995; Larsson *et al.*, 1995) and has been found to interact with splice factors *in vivo* (Ladomery *et al.*, 1999). Furthermore, both isoforms shuttle between the nucleus and cytoplasm and are associated with functional polysomes (Niksic *et al.*, 2004). Both isoforms have been found to interact with the splice factor U2AF65 (Davies *et al.*, 1998) which is associated with nuclear mRNP particles. Both isoforms of WT1 can specifically bind to RNA sequences *in vitro* (Caricasole *et al.*, 1996; Bardeesy and Pelletier, 1998); however, no *in vivo* target has been isolated to date.

Although there has been no *in vivo* mRNA target for WT1, the evidence presented above suggests that an mRNA target does exist, and that understanding of this interaction will provide a clearer picture of the involvement of WT1 in development and disease. With the current lack of a crystal structure of WT1 bound to a RNA ligand, it is important to develop other methods of elucidating the mechanism of this interaction. In the current study, a nitrocellulose filter binding assay was employed to probe the interaction of WT1 with its specific RNA ligand

Pel22. Filter binding experiments have been used in the past by our lab to investigate both the DNA and RNA binding activities of the zinc finger proteins TFIIIA and WT1 and the RNA binding activities of the zinc finger protein p43 (Romaniuk, 1985; Romaniuk, 1990; Hamilton *et al.*, 1995; Zang and Romaniuk, 1995; Zang *et al.*, 1995; Borel *et al.*, 1996; Hamilton *et al.*, 1997; Hamilton *et al.*, 1998; Hamilton *et al.*, 2001; Zhai *et al.*, 2001).

It was hypothesized that like both TFIIIA and p43, specific amino acid residues of the zinc finger region of WT1 significantly contribute to RNA binding. Swapping these residues with sequences from donor zinc finger peptides provided an experimental context for identifying amino acid residues important for RNA binding with mutants of WT1 that would maintain the tertiary structure of the zinc finger domain.

4.1. WT1 -TFIIIA 4-7 swap mutants

Initially, a set of 4 WT1 +KTS mutants were constructed using the cDNA sequence from TFIIIA zinc fingers 4-7. The basis for using TFIIIA 4-7 as a donor came from experiments where fingers 4-7 of TFIIIA were replaced with WT1 zinc fingers in the full length zinc finger region of TFIIIA (Hamilton *et al.*, 2001). These experiments demonstrated that when fingers 4-7 are replaced by WT1, the protein can no longer bind to its specific RNA ligand 5S RNA, and the protein acquires the ability to bind to the WT1 specific ligand Pel22. Furthermore, the evidence presented by the solved crystal structure of zinc fingers 4-6 of TFIIIA interacting with a truncated version of 5S RNA (Lu *et al.*, 2003) indicated that the finger interactions with the RNA molecule were mediated through residues located in the α helical

region of the zinc finger. Past studies of WT1-RNA interactions have demonstrated that the zinc finger region alone was sufficient to confer RNA binding specificity (Bardeesy and Pelletier, 1998; Zhai *et al.*, 2001). With this and the evidence presented above in mind, WT1 zinc finger mutants were constructed with the α-helix replaced with regions of the TFIIIA 4-7 protein, encoding for 4 mutant proteins containing only the zinc finger region of WT1. The α helix of finger 1 of WT1 was replaced by the α helix of finger 4 of TFIIIA, the α helix of finger 2 of WT1 was replaced by the α helix of finger 5 of TFIIIA, the α helix of finger 3 of WT1 was replaced by the α helix of finger 6 of TFIIIA and the α helix of finger 4 of WT1 was replaced with the α helix of finger 7 of TFIIIA (Figure 7).

Results from filter-binding assays of these 4 mutants with the specific WT1 RNA aptamer Pel22, demonstrated only modest differences in affinity for Pel22 in comparison to wild type WT1 +KTS ZF binding. Two of the mutants showed approximately a 1.5-2X decrease in binding affinity, which included the mutant Wx1B+ , which had the α-helix of finger 1 swapped with the α-helix of finger 4 of TFIIIA, and the Wx2B+ mutant which had the α-helix of finger 2 swapped with the α-helix of finger 5 of TFIIIA. The other two mutants, Wx3B+ that has the α-helix of finger 3 replaced with the α-helix of finger 6 of TFIIIA, and Wx4B+ that has the α-helix of finger 4 replaced with the α-helix of finger 7 of TFIIIA showed a slight increase in affinity for Pel22, by approximately 1.5X. The results from these experiments were quite unexpected. In an attempt to analyze any possible differences between these mutants and wild type WT1, another set of binding experiments were preformed to test the ability of the mutants to bind to a non-specific RNA, 5S RNA.

Wild type WT1 does not bind to 5S RNA with any appreciable affinity exhibiting a K_d value of over 1000 nM. Filter binding of the mutants with 5S RNA indicated that both the Wx1B+ and Wx2B+ behaved in similar manner to wild type with respect to both Pel22 (specific ligand) and 5S RNA (non-specific ligand). Interestingly, both the Wx3B+ and Wx4B+ were able to bind to 5S RNA with 4 and 12 times higher affinity that wild type respectively. However, both still demonstrated similar binding affinities as wild type for Pel22.

There are two possible scenarios that would explain why none of the mutants showed a decrease in binding affinity for Pel22. Either WT1 RNA binding is not mediated through the α helices, or the protein residues that we replaced each region of the zinc fingers with actually have the ability to bind to Pel22. In order to test for the latter, which was the most easily done, we used a nitrocellulose filter binding assay to evaluate the ability of the TFIIIA 4-7 portion of TFIIIA to bind to Pel22. To our surprise, this peptide was able to bind to Pel22 with an affinity only 2-3X lower than the affinity of WT1 for the ligand. While Pel22 was selected by exponential enrichment (SELEX) using WT1 (Bardeesy and Pelletier, 1998), and experiments have shown that the Pel22-WT1 interaction is specific as WT1-Pel22 affinity is not competed out by unrelated RNA sequences of the same length as Pel22; there have not been experiments to test the ability of other zinc finger proteins to bind to Pel22. Although the experiments were not published, the authors did mention that EGR-1 could also bind Pel22 and suggested that zinc finger proteins with high homology to WT1 may also be able to bind to this sequence (Bardeesy and Pelletier, 1998);

however, they most likely underestimated specificity of Pel22 for other non-homologous zinc finger proteins .

Although the results from the TFIIIA swap mutants were uninformative in indicating which finger of WT1 is involved in the specific WT1-Pel22 interaction, these experiments have brought to light the capabilities of Pel22 to bind to other zinc finger proteins, and the importance of choosing donor peptide sequences that cannot bind to this RNA. Interestingly, the Wx4B+ mutant did demonstrate a difference in binding affinity for the non-specific WT1 ligand 5S RNA. While the fact that TFIIIA 4-7 itself binds to 5S RNA makes the finding that this mutant can also bind to 5S RNA a non-definitive result, there has been no evidence to suggest that finger 7 plays a crucial role in the binding of TFIIIA to 5S RNA. This result certainly suggests that finger 4 confers an important function in the binding of WT1 to RNA. However, the poor choice of donor peptide in these experiments makes it impossible to draw a clear conclusion as to the exact role of finger 4 in RNA binding.

4.2. WT1-p43 swap mutants

The results from the TFIIIA4-7 swap mutants exemplified the importance of choosing an appropriate donor peptide and testing it to make sure it does not bind to Pel22 itself. Filter binding experiments with the peptide p43 6-9 which contains only fingers 6 through 9 of p43, demonstrated that this peptide does not bind with any sort of specificity to Pel22 or 5S RNA making it an acceptable donor sequence for further probing experiments.

A series of p43 swap mutants, and two WT1 deletion mutants were created to try and determine which zinc finger of WT1 was the most crucial in mediating the

specific WT1 Pel22 interaction. The first set of p43 swap mutants replaced fingers 1, 1 and 2, 3 and 4 and 4 with fingers 6, 6 and 7, 8 and 9, and 9 of p43 respectively. The mutant Wp4, which has finger 4 of WT1 replaced with finger 9 of p43, demonstrated a 10X higher affinity for Pel22 than wild type WT1. The mutant Wp3-4, which has zinc fingers 3 and 4 of WT1 replaced with fingers 8 and 9 of p43 demonstrated approximately 6X lower affinity for Pel22 when compared to wild type. When comparing the affinities for Pel22 between the Wp3-4 and Wp4 mutants, we see a 60 fold decrease in affinity for Pel22 by the Wp3-4 mutant. This prompted us to construct another mutant, W12P8W4, in which finger 3 of WT1 was replaced by finger 8 of p43. Experiments with this protein demonstrated that replacement of finger three confers at least a 5-10 fold reduction in affinity for Pel22; however, the curve used to extrapolate the binding dissociation constant of this protein did not reach the plateau so it is hard to say whether it is more than 10 fold down, which is possible. Due to limitations within the filter binding assay, it was not possible to include higher protein concentrations within the experiment because wild type WT1 showed a decrease in Pel22 affinity at these higher concentrations.

There has been conflicting evidence in the literature on whether finger 1 or finger 4 is most crucial for WT1 RNA interaction. WT1 deletion mutants were created that either had finger 1 or finger 4 missing. Results from filter binding experiments explicitly show that when finger 4 is deleted this results in almost no binding to Pel22. On the other hand, deletion of finger 1 results in no difference in affinity for Pel22. Although these results do demonstrate that finger 4 plays a role in RNA binding, it is possible that finger 4 is not making specific base contacts with the

RNA because the finger 4 swap mutant didn't show this decrease in affinity, and actually bound to Pel22 with higher affinity. However, when analyzing the equilibrium binding of Wp4, it can be seen that the data points do not fit the predicted bimolecular equilibrium curve, indicating that this mutant may bind to Pel22 in another manner. Interestingly, the finger 4 swap mutant Wp4, was the only mutant that demonstrated an increased interaction with 5S RNA, having a 55X higher affinity compared to the wild type WT1-5S RNA binding affinity. This result indicates that Wp4 has lost specificity for Pel22. There are a couple of hypothesis as for these results and the function of finger 4. One possibility is that finger 4 of WT1 it is involved in the stabilization of the RNA complex. It is possible that finger 9 of p43 co-ordinates zinc more strongly than finger 4 of WT1, and is able to provide more stability to the protein-RNA complex. This hypothesis would also explain the 100-fold decrease in affinity of WT1 for Pel22 when finger 4 is completely deleted. If finger 4 is the major contributor to the stabilization of the protein-RNA complex, its removal would result in dissociation of the complex. Another possibility is that when finger 4 of WT1 is replaced with finger 9 of p43, this alters the mechanism of WT1-Pel22 binding and the binding kinetics no longer follow the simple bimolecular model.

4.3. Comparison to previous studies on WT1 zinc finger roles

There is an ongoing debate over which finger is most crucial for WT1-RNA interaction. To date, the only published data involves analyzing WT1-RNA specificity by deleting either finger 1 or finger 4 of the zinc finger region, and analyzing these mutants this using qualitative binding assays (Caricasole *et al.*, 1996;

Bardeesy and Pelletier, 1998). In the gel shift assay in which the WT1 specific RNA aptamer Pel22 was selected, it was found that finger 1 deletions of WT1 had minor effects on the affinity of the protein for Pel22, while deletion of finger 4 resulted in ablation of RNA binding affinity (Bardeesy and Pelletier, 1998). Our results from this study agree with these results, and take the analysis further by quantitating the relative affinities of each mutant for Pel22 compared to the wild type WT1.

Another study has shown that both the +KTS and –KTS WT1 isoforms can bind to the RNA sequence derived from exon 2 sequences of the mouse gene encoding insulin-like growth factor 2 (Igf-2) (Caricasole *et al.*, 1996). In these experiments it was shown by a qualitative gel shift assay that deletion of finger 1 resulted in ablation of RNA binding specificity and that deletion of finger 4 had minimal effects on RNA binding affinity. It is possible that the binding of WT1 to exonic Igf-2 RNA sequence is a different mode of binding than that of WT1-Pel22 RNA binding; however, it is important to take into consideration that in the Igf-2 experiments a non-quantitative assay was used, in comparison with the filter binding assay, which quantitatively determines binding dissociation constants. Unpublished results from our laboratory have demonstrated that the interaction of WT1 with the Igf-2 RNA is nonspecific; any RNA of similar length binds with the same affinity as Igf-2.

It is also important to keep in mind that experiments such as this, that involved large deletions of the WT1 protein, are not as informative as swap mutants. Deletion of an entire zinc finger could alter the stability of the protein, and it is possible that these large deletions could still result in a decrease in affinity for RNA

in cases where specific amino-acid base contacts are not occuring by disrupting the overall stability of the protein-RNA complex.

4.4. Possible finger-finger interactions in the mode of WT1-RNA binding

The results from this study raise some very interesting questions about the possibility of WT1 zinc finger 4 playing a major role in the stabilization of the WT1-RNA complex by perhaps conferring more stability to the other three fingers of the protein. It seems as though finger 4 is indeed important in the WT1-Pel22 interaction, since when it is deleted, RNA binding is ablated. The results with the finger swapping mutants suggest that it is not making residue specific contacts with the RNA as demonstrated by an actual increase in binding by Wp4. On the other hand, results from these experiments clearly indicate a role for finger 3 of WT1 in binding to Pel22 RNA, which when replaced with finger 8 of p43, results in at least a 5 fold decrease in binding affinity. The combined results suggest that finger 3 is making residue specific contacts with the RNA, and that possibly in some way other than specific residue contacts, zinc finger 4 of WT1 is responsible for the stability of the WT1-RNA complex.

WT1 is a notable example of a zinc finger protein that can bind to both types of nucleic acids, DNA and RNA. At this point in time, only the biological significance of DNA binding by WT1 is known. Although there is an abundance of evidence to suggest a possible role for the +KTS isoform in mRNA processing, an *in vivo* cellular RNA target has yet to be identified. The finding that the WT1 –KTS isoform binds to DNA, while +KTS isoform does not, suggests that the mode of DNA and RNA binding by WT1 is distinct. This study has demonstrated that in the WT1-

RNA interaction, residues within finger 3 are most crucial to this interaction. It is possible that these findings will lead to experiments that narrow down which residues are specifically responsible for the RNA interaction, and these mutants could be used to elucidate the biological role of this protein in development and disease.

4.5. Future Directions

The results from this study represent advancement in the understanding of interaction of WT1 with its specific ligand Pel22. In future experiments it may be possible to determine which residues within zinc finger 3 are specifically responsible for the Pel22 RNA interaction. It would also be interesting to construct the same mutants in +KTS to see if zinc finger 3 in this isoform is also making specific amino acid contacts in RNA binding.

As previously mentioned, it appears as though the DNA and RNA binding capabilities of the WT1 protein are distinct. Therefore, these mutants would be very useful for *in vivo* studies that could lead to elucidating the biological role of the protein. Also, these mutants could be used to probe WT1 interactions with other proteins *in vitro* and *in vivo*.

Chapter 5. Conclusion

WT1 is a multifunctional protein that has both the ability to bind to DNA and RNA *in vitro* (Rauscher *et al.*, 1990; Bardeesy and Pelletier, 1998). The two main isoforms of this protein +KTS and –KTS have different nucleic acid binding specificities. While +KTS can only bind to RNA with high affinity and in a sequence specific manner, the –KTS isoform can bind both to DNA and RNA in this manner (Zhai *et al.*, 2001). Not surprisingly, the –KTS form of the protein functions as a transcription factor, and although it can also bind to RNA and is found in functional polysomes (Niksic *et al.*, 2004), it is thought that transcriptional regulation is its primary function. As far as the +KTS isoform is concerned, its function can only be hypothesized, and evidence suggests that it may be involved in mRNA processing.

The present study has analyzed the WT1 interaction with its specific RNA ligand Pel22 in a quantitative manner in order to determine which zinc finger of WT1 is most crucial in binding to RNA. The results clearly demonstrate a role for finger 3 in WT1-Pel22 binding, and also implicate finger 4 as a possible major contributor to WT1-RNA complex stabilization. While the effects of both p43 swap mutants and WT1 deletion mutants are informative and promising, a complete understanding of WT1-RNA interaction will most likely have to wait until the complex has been solved by x-ray crystallography. It is hoped that the findings of this study will aid in further research into the role of this protein in human disease and development, and that further experiments will shed light on the increasingly complex networks in which WT1 is found to be involved.

Literature Cited

Ambion. MAXIscript In Vitro Transcription Kit. MAXIscript Manual: 5.

Armstrong, J. F., K. Pritchard-Jones, W. A. Bickmore, N. D. Hastie and J. B. Bard (1993). "The expression of the Wilms' tumour gene, WT1, in the developing mammalian embryo." Mech Dev **40**(1-2): 85-97.

Barbaux, S., P. Niaudet, M. C. Gubler, J. P. Grunfeld, F. Jaubert, F. Kuttenn, C. N. Fekete, N. Souleyreau-Therville, E. Thibaud, M. Fellous and K. McElreavey (1997). "Donor splice-site mutations in WT1 are responsible for Frasier syndrome." Nat Genet **17**(4): 467-70.

Bardeesy, N. and J. Pelletier (1998). "Overlapping RNA and DNA binding domains of the wt1 tumor suppressor gene product." Nucleic Acids Res **26**(7): 1784-92.

Barrett, P., P.-M. Kloetzel and J. Sommerville (1983). "Specific interaction of proteins with 5S RNA and tRNA in the 42S storage particle of *Xenopus* oocytes." Biochim. Biophys. Acta **740**: 347-354.

Bickmore, W. A., K. Oghene, M. H. Little, A. Seawright, V. van Heyningen and N. D. Hastie (1992). "Modulation of DNA binding specificity by alternative splicing of the Wilms tumor wt1 gene transcript." Science **257**(5067): 235-7.

Borel, F., K. C. Barilla, T. B. Hamilton, M. Iskandar and P. J. Romaniuk (1996). "Effects of Denys-Drash syndrome point mutations on the DNA binding activity of the Wilms' tumor suppressor protein WT1." Biochemistry **35**(37): 12070-12076.

Brown, K. W. and K. T. Malik (2001). "The molecular biology of Wilms tumour." Expert Rev Mol Med **2001**: 1-16.

Brown, R. S. (2005). "Zinc finger proteins: getting a grip on RNA." Curr Opin Struct Biol **15**(1): 94-8.

Bruening, W. and J. Pelletier (1996). "A non-AUG translational initiation event generates novel WT1 isoforms." J. Biol. Chem. **271**: 8646-8654.

Call, K. M., T. Glaser, C. Y. Ito, A. J. Buckler, J. Pelletier, D. A. Haber, E. A. Rose, A. Kral, H. Yeger, W. H. Lewis, C. Jones and D. E. Housman (1990). "Isolation and Characterization of a Zinc Finger Polypeptide Gene at the Human Chromosome-11 Wilms Tumor Locus." Cell **60**(3): 509-520.

Carey, J. and O. C. Uhlenbeck (1983). "Kinetic and Thermodynamic Characterization of the R17 Coat Protein-Ribonucleic Acid Interaction." Biochemistry **22**: 2610-2615.

Caricasole, A., A. Duarte, S. H. Larsson, N. D. Hastie, M. Little, G. Holmes, I. Todorov and A. Ward (1996). "RNA binding by the Wilms tumor suppressor zinc finger proteins." Proceedings of the National Academy of Sciences U.S.A. **93**: 7562-7566.

Cassiday, L. A. and L. J. Maher, 3rd (2002). "Having it both ways: transcription factors that bind DNA and RNA." Nucleic Acids Res **30**(19): 4118-26.

Charlieu, J.-P., S. Larsson, K. Miyagawa, V. van Heyningen and N. D. Hastie (1995). "Does the Wilms' tumour suppressor gene WT1, play roles in both splicing and transcription." J. Cell. Sci. **Supp. 19**: 95-99.

Choo, Y. and A. Klug (1993). "A role in DNA binding for the linker sequences of the 1st 3 zinc fingers of TFIIIA." Nucleic Acids Res **21**(15): 3341-3346.

Clemens, K. R., V. Wolf, S. J. Mcbryant, P. H. Zhang, X. B. Liao, P. E. Wright and J. M. Gottesfeld (1993). "Molecular basis for specific recognition of both RNA and DNA by a zinc finger protein." Science **260**(5107): 530-533.

Cook, D. M., M. T. Hinkes, M. Bernfield and F. J. Rauscher, 3rd (1996). "Transcriptional activation of the syndecan-1 promoter by the Wilms' tumor protein WT1." Oncogene **13**(8): 1789-99.

Corbi, N., V. Libri, A. Onori and C. Passananti (2004). "Synthetic zinc finger peptides: old and novel applications." Biochem Cell Biol **82**(4): 428-36.

Davies, J. A., M. Ladomery, P. Hohenstein, L. Michael, A. Shafe, L. Spraggon and N. Hastie (2004). "Development of an siRNA-based method for repressing specific genes in renal organ culture and its use to show that the Wt1 tumour suppressor is required for nephron differentiation." Hum Mol Genet **13**(2): 235-46.

Davies, R. C., C. Calvio, E. Bratt, S. H. Larsson, A. I. Lamond and N. D. Hastie (1998). "WT1 interacts with the splicing factor U2AF65 in an isoform-dependent manner and can be incorporated into spliceosomes." Genes Dev **12**(20): 3217-25.

Denis, H. and M. Mairy (1972). "Recherches biochimiques sur l'oogenese." Eur. J. Biochem. **25**: 524-534.

Dillon, P. J. and C. A. Rosen (1990). "A rapid method for the construction of synthetic genes using the polymerase chain reaction." Biotechniques **9**(3): 298, 300.

Discenza, M. T. and J. Pelletier (2004). "Insights into the physiological role of WT1 from studies of genetically modified mice." Physiol Genomics **16**(3): 287-300.

Drummond, I. A., H. D. Rupprecht, P. Rohwernutter, J. M. Lopezguisa, S. L. Madden, F. J. Rauscher and V. P. Sukhatme (1994). "DNA recognition by splicing variants of the wilms' tumor suppressor, WT1." Mol Cell Biol **14**(6): 3800-3809.

Fearon, B., V. Forte and I. Brama (1990). "Malignant nasopharyngeal tumors in children." Laryngoscope **100**(5): 470-2.

Francke, U., L. B. Holmes, L. Atkins and V. M. Riccardi (1979). "Aniridia-Wilms' tumor association: evidence for specific deletion of 11p13." Cytogenet Cell Genet **24**(3): 185-92.

Gashler, A. L., D. T. Bonthron, S. L. Madden, F. J. Rauscher, T. Collins and V. P. Sukhatme (1992). "Human Platelet-Derived growth Factor-A chain is transcriptionally repressed by the wilms tumor suppressor WT1." Proc Natl Acad Sci USA **89**(22): 10984-10988.

Guo, J. K., A. L. Menke, M. C. Gubler, A. R. Clarke, D. Harrison, A. Hammes, N. D. Hastie and A. Schedl (2002). "WT1 is a key regulator of podocyte function: reduced expression levels cause crescentic glomerulonephritis and mesangial sclerosis." Hum Mol Genet **11**(6): 651-9.

Haber, D. A., A. J. Buckler, T. Glaser, K. M. Call, J. Pelletier, R. L. Sohn, E. C. Douglass and D. E. Housman (1990). "An Internal Deletion Within an 11P13 Zinc Finger Gene Contributes to the Development of Wilms Tumor." Cell **61**(7): 1257-1269.

Haber, D. A., R. L. Sohn, A. J. Buckler, J. Pelletier, K. M. Call and D. E. Housman (1991). "Alternative splicing and genomic structure of the Wilms tumor gene WT1." Proc Natl Acad Sci U S A **88**(21): 9618-22.

Hall, T. M. (2005). "Multiple modes of RNA recognition by zinc finger proteins." Curr Opin Struct Biol **15**(3): 367-73.

Hamilton, T., K. Barilla and P. Romaniuk (1995). "High affinity binding sites for the Wilms' tumour suppressor protein WT1." Nucl Acids Res **23**: 277-284.

Hamilton, T., F. Borel and P. J. Romaniuk (1997). "Comparison of the DNA Binding Characteristics of the Related Zinc Finger Proteins WT1 and EGR1." Biochemistry **submitted**.

Hamilton, T. B., K. C. Barilla and P. J. Romaniuk (1995). "High affinity binding sites for the Wilms' tumour suppressor protein WT1." Nucleic Acids Res **23**(2): 277-84.

Hamilton, T. B., F. Borel and P. J. Romaniuk (1998). "Comparison of the DNA binding characteristics of the related zinc finger proteins WT1 and EGR1." Biochemistry **37**(7): 2051-8.

Hamilton, T. B., J. Turner, K. Barilla and P. J. Romaniuk (2001). "Contribution of individual amino acids to the nucleic acid binding activities of the Xenopus zinc finger proteins TFIIIIA and p43." Biochemistry **40**(20): 6093-101.

Hewitt, S. M., S. Hamada, T. J. McDonnell, F. J. Rauscher and G. F. Saunders (1995). "Regulation of the proto-oncogenes bcl-2 and c-myc by the Wilms' tumor suppressor gene WT1." Cancer Res. **55**: 5386-5389.

Hirose, M. (1999). "The role of Wilms' tumor genes." J Med Invest **46**(3-4): 130-40.

Holbrook, S. R. (2005). "RNA structure: the long and the short of it." Curr Opin Struct Biol **15**(3): 302-8.

Hosono, S., I. Gross, M. A. English, K. M. Hajra, E. R. Fearon and J. D. Licht (2000). "E-cadherin is a WT1 target gene." J Biol Chem **275**(15): 10943-53.

Invitrogen. (2003). "pCR T7 TOPO TA expression Kits". Invitrogen **I**: 11-22.

Iuchi, S. (2001). "Three classes of C2H2 zinc finger proteins." Cell Mol Life Sci **58**(4): 625-35.

Johnstone, R. W., R. H. See, S. F. Sells, J. Wang, S. Muthukkumar, C. Englert, D. A. Haber, J. D. Licht, S. P. Sugrue, T. Roberts, V. M. Rangnekar and Y. Shi (1996). "A novel repressor, par-4, modulates transcription and growth suppression functions of the Wilms' tumor suppressor WT1." Mol. Cell. Biol. **16**: 6945-6956.

Johnstone, R. W., J. Wang, N. Tommerup, H. Vissing, T. Roberts and Y. Shi (1998). "Ciao 1 is a novel WD40 protein that interacts with the tumor suppressor protein WT1." J Biol Chem **273**(18): 10880-7.

Jones, S., D. T. Daley, N. M. Luscombe, H. M. Berman and J. M. Thornton (2001). "Protein-RNA interactions: a structural analysis." Nucleic Acids Res **29**(4): 943-54.

Joseph, L. J., M. M. le Beau, G. A. J. Jamieson, S. Acharya, T. B. Shows, J. D. Rowley and V. P. Sukhatme (1988). "Molecular cloning, sequencing, and mapping of *EGR2*, a human early growth response gene encoding a protein with "zinc-binding finger" structure." Proc. Natl. Acad. Sci. USA **85**(10): 7164-7168.

Ke, A. and J. A. Doudna (2004). "Crystallization of RNA and RNA-protein complexes." Methods **34**(3): 408-14.

Kent, J., A. M. Coriat, P. T. Sharpe, N. D. Hastie and V. van Heyningen (1995). "The evolution of WT1 sequence and expression pattern in the vertebrates." Oncogene **11**(9): 1781-92.

Klamt, B., A. Koziell, F. Poulat, P. Wieacker, P. Scambler, P. Berta and M. Gessler (1998). "Frasier syndrome is caused by defective alternative splicing of WT1 leading to an altered ratio of WT1 +/-KTS splice isoforms." Hum Mol Genet **7**(4): 709-14.

Kohsaka, T., M. Tagawa, Y. Takekoshi, H. Yanagisawa, K. Tadokoro and M. Yamada (1999). "Exon 9 mutations in the WT1 gene, without influencing KTS splice isoforms, are also responsible for Frasier syndrome." Hum Mutat **14**(6): 466-70.

Kreidberg, J. A., H. Sariola, J. M. Loring, M. Maeda, J. Pelletier, D. Housman and R. Jaenisch (1993). "WT-1 is required for early kidney development." Cell **74**(4): 679-691.

Krishna, S. S., I. Majumdar and N. V. Grishin (2003). "Structural classification of zinc fingers: survey and summary." Nucleic Acids Res **31**(2): 532-50.

Ladomery, M. R., J. Slight, S. Mc Ghee and N. D. Hastie (1999). "Presence of WT1, the Wilm's tumor suppressor gene product, in nuclear poly(A)(+) ribonucleoprotein." J Biol Chem **274**(51): 36520-6.

Laity, J. H., H. J. Dyson and P. E. Wright (2000). "DNA-induced alpha-helix capping in conserved linker sequences is a determinant of binding affinity in Cys(2)-His(2) zinc fingers." J Mol Biol **295**(4): 719-27.

Laity, J. H., B. M. Lee and P. E. Wright (2001). "Zinc finger proteins: new insights into structural and functional diversity." Curr Opin Struct Biol **11**(1): 39-46.

Larsson, S. H., J.-P. Charlieu, K. Miyagawa, D. Engelkamp, M. Rassoulzadegan, A. Ross, F. Cuzin, V. van Heyningen and N. D. Hastie (1995). "Subnuclear localization of WT1 in splicing or transcription factor domains is regulated by alternative splicing." Cell **81**: 391-401.

Lee, S. B. and D. A. Haber (2001). "Wilms tumor and the WT1 gene." Exp Cell Res **264**(1): 74-99.

Lee, S. B., K. Huang, R. Palmer, V. B. Truong, D. Herzlinger, K. A. Kolquist, J. Wong, C. Paulding, S. K. Yoon, W. Gerald, J. D. Oliner and D. A. Haber (1999). "The Wilms tumor suppressor WT1 encodes a transcriptional activator of amphiregulin." Cell **98**(5): 663-73.

Little, M. and C. Wells (1997). "A clinical overview of WT1 gene mutations." Hum Mutat **9**(3): 209-25.

Little, M. H., K. A. Williamson, M. Mannens, A. Kelsey, C. Gosden, N. D. Hastie and V. Vanheyningen (1993). "Evidence that WT1 mutations in Denys-Drash syndrome patients may act in a Dominant-Negative fashion." Hum Mol Genet **2**(3): 259-264.

Lu, D., M. A. Searles and A. Klug (2003). "Crystal structure of a zinc-finger-RNA complex reveals two modes of molecular recognition." Nature **426**(6962): 96-100.

Madden, S. L., D. M. Cook, J. F. Morris, A. Gashler, V. P. Sukhatme and F. J. Rauscher (1991). "Transcriptional Repression Mediated by the WTI Wilms Tumor Gene Product." Science **253**(5027): 1550-1553.

Maheswaran, S., C. Englert, P. Bennett, G. Heinrich and D. A. Haber (1995). "The WT1 gene product stabilizes p53 and inhibits p53-mediated apoptosis." Genes & Devel. **9**: 2143-2156.

Maheswaran, S., S. Park, A. Bernard, J. F. Morris, F. J. Rauscher, D. E. Hill and D. A. Haber (1993). "Physical and functional interaction between WT1 and p53 proteins." Proc Natl Acad Sci USA **90**(11): 5100-5104.

Malik, K. T. A., V. Poirier, S. M. Ivins and K. W. Brown (1994). "Autoregulation of the human WT1 gene promoter." FEBS Lett **349**(1): 75-78.

Matsunaga, E. (1982). "Cancer susceptibility: family studies of retinoblastoma and Wilms tumor." Prog Clin Biol Res **103 Pt B**: 241-9.

McBryant, S. J., N. Veldhoen, B. Gedulin, A. Leresche, M. P. Foster, P. E. Wright, P. J. Romaniuk and J. M. Gottesfeld (1995). "Interaction of the RNA binding fingers of Xenopus transcription factor IIIA with specific regions of 5 S ribosomal RNA." J Mol Biol **248**(1): 44-57.

McTaggart, S. J., E. Algar, C. W. Chow, H. R. Powell and C. L. Jones (2001). "Clinical spectrum of Denys-Drash and Frasier syndrome." Pediatr Nephrol **16**(4): 335-9.

Metzger, M. L. and J. S. Dome (2005). "Current therapy for Wilms' tumor." Oncologist **10**(10): 815-26.

Miles, C. G., L. Rankin, S. I. Smith, M. Niksic, G. Elgar and N. D. Hastie (2003). "Faithful expression of a tagged Fugu WT1 protein from a genomic transgene in zebrafish: efficient splicing of pufferfish genes in zebrafish but not mice." Nucleic Acids Res **31**(11): 2795-802.

Miller, J., A. D. McLachlan and A. Klug (1985). "Repetitive zinc-binding domains in the protein transcription factor IIIA from Xenopus oocytes." EMBO J. **4**: 1609-1614.

Miyagawa, K., Y. Hayashi, T. Fukuda, K. Mitani, H. Hirai and K. Kamiya (1999). "Mutations of the WT1 gene in childhood nonlymphoid hematological malignancies." Genes Chromosomes Cancer **25**(2): 176-83.

Morris, J. F., S. L. Madden, O. E. Tournay, D. M. Cook, V. P. Sukhatme and F. J. Rauscher (1991). "Characterization of the Zinc Finger Protein Encoded by the WT1 Wilms' Tumor Locus." Oncogene **6**(12): 2339-2348.

Nakagama, H., G. Heinrich, J. Pelletier and D. E. Housman (1995). "Sequence and structural requirements for high-affinity DNA binding by the WT1 gene product." Mol Cell Biol **15**(3): 1489-98.

Niksic, M., J. Slight, J. R. Sanford, J. F. Caceres and N. D. Hastie (2004). "The Wilms' tumour protein (WT1) shuttles between nucleus and cytoplasm and is present in functional polysomes." Hum Mol Genet **13**(4): 463-71.

Nyman, U., H. Hallman, G. Hadlaczky, I. Pettersson, G. Sharp and N. R. Ringertz (1986). "Intranuclear localization of snRNP antigens." J Cell Biol **102**(1): 137-44.

Oji, Y., Y. Miyoshi, E. Kiyotoh, S. Koga, Y. Nakano, A. Ando, N. Hosen, A. Tsuboi, M. Kawakami, K. Ikegame, Y. Oka, H. Ogawa, S. Noguchi and H. Sugiyama (2004). "Absence of mutations in the Wilms' tumor gene WT1 in primary breast cancer." Jpn J Clin Oncol **34**(2): 74-7.

Orkin, S. H., D. S. Goldman and S. E. Sallan (1984). "Development of homozygosity for chromosome 11p markers in Wilms' tumour." Nature **309**(5964): 172-4.

Pabo, C. O., E. Peisach and R. A. Grant (2001). "Design and selection of novel Cys2His2 zinc finger proteins." Annu Rev Biochem **70**: 313-40.

Pavletich, N. P. and C. O. Pabo (1991). "Zinc Finger-DNA Recognition - Crystal Structure of a Zif268-DNA Complex at 2.1-A." Science **252**(5007): 809-817.

Pelletier, J., W. Bruening, C. E. Kashtan, S. M. Mauer, J. C. Manivel, J. E. Striegel, D. C. Houghton, C. Junien, R. Habib, L. Fouser, R. N. Fine, B. L. Silverman, D. A. Haber and D. Housman (1991). "Germline Mutations in the Wilms' Tumor Suppressor Gene Are Associated with Abnormal Urogenital Development in Denys-Drash Syndrome." Cell **67**(2): 437-447.

Pendergrass, T. W. (1976). "Congenital anomalies in children with Wilms' tumor: a new survey." Cancer **37**(1): 403-8.

Qiagen. (2002). "QIAquick spin handbook." Qiagen: 18

Qiagen (2002). QIAprep miniprep handbook."Qiagen: 22-23.

Rauscher, F. J., J. F. Morris, O. E. Tournay, D. M. Cook and T. Curran (1990). "Binding of the Wilms Tumor Locus Zinc Finger Protein to the Egr-1 Consensus Sequence." Science **250**(4985): 1259-1262.

Riccardi, V. M., E. Sujansky, A. C. Smith and U. Francke (1978). "Chromosomal imbalance in the Aniridia-Wilms' tumor association: 11p interstitial deletion." Pediatrics **61**(4): 604-10.

Romaniuk, P. J. (1985). "Characterization of the RNA binding properties of transcription factor IIIA of *Xenopus laevis* oocytes." Nucl. Acids Res. **13**(14): 5369-5387.

Romaniuk, P. J. (1989). "The role of highly conserved single-stranded nucleotides of *Xenopus* 5S RNA in the binding of transcription factor IIIA." Biochemistry **28**: 1388-1395.

Romaniuk, P. J. (1990). "Characterization of the Equilibrium Binding of *Xenopus* Transcription Factor IIIA to the 5S RNA Gene." J Biol Chem **265**(29): 17593-17600.

Romaniuk, P. J., I. L. de Stevenson and H.-H. A. Wong (1987). "Defining the binding site of *Xenopus* transcription factor IIIA on 5S RNA using truncated and chimeric 5S RNA molecules." Nucl. Acids Res. **15**(6): 2737-2755.

Romaniuk, P. J., I. L. de Stevenson and Q. You, Eds. (1989). The specificity of the RNA binding activity of Xenopus transcription factor IIIA. Molecular Biology of RNA. New York, Alan R. Liss, Inc.

Rupprecht, H. D., I. A. Drummond, S. L. Madden, F. J. Rauscher and V. P. Sukhatme (1994). "The wilms tumor suppressor gene wt1 is negatively autoregulated." J Biol Chem **269**(8): 6198-6206.

Saylam, K. and P. Simon (2003). "WT1 gene mutation responsible for male sex reversal and renal failure: the Frasier syndrome." Eur J Obstet Gynecol Reprod Biol **110**(1): 111-3.

Scharnhorst, V., P. Dekker, A. J. van der Eb and A. G. Jochemsen (1999). "Internal translation initiation generates novel WT1 protein isoforms with distinct biological properties." J Biol Chem **274**(33): 23456-62.

Spector, D. L., X. D. Fu and T. Maniatis (1991). "Associations between distinct pre-mRNA splicing components and the cell nucleus." Embo J **10**(11): 3467-81.

Sukhatme, V. P., X. Cao, L. C. Chang, C. H. Tsai-Morris, D. Stamenkovich, P. C. P. Ferreira, D. R. Cohen, S. A. Edwards, T. B. Shows, T. Curran, M. M. Le Beau and E. D. Adamson (1988). "A zinc finger-encoding gene coregulated w ith c-fos during growth and differentiation, and after cellular depolarization ." Cell **53**: 37-43.

Venter, J. C., M. D. Adams, E. W. Myers, P. W. Li, R. J. Mural, G. G. Sutton, H. O. Smith, M. Yandell, C. A. Evans, R. A. Holt, J. D. Gocayne, P. Amanatides, R. M. Ballew, D. H. Huson, J. R. Wortman, Q. Zhang, C. D. Kodira, X. H. Zheng, L. Chen, M. Skupski, *et al.* (2001). "The sequence of the human genome." Science **291**(5507): 1304-51.

Wagner, K. D., N. Wagner and A. Schedl (2003). "The complex life of WT1." J Cell Sci **116**(Pt 9): 1653-8.

Wang, Z. Y., S. L. Madden, T. F. Deuel and F. J. Rauscher (1992). "The wilms' tumor gene product, WT1, represses transcription of the Platelet-Derived growth factor A-Chain gene." J Biol Chem **267**(31): 21999-22002.

Wang, Z. Y., Q. Q. Qiu, J. Huang, M. Gurrieri and T. F. Deuel (1995). "Products of alternatively spliced transcripts of the Wilms' tumor suppressor gene, wt1, have altered DNA binding specificity and regulate transcription in different ways." Oncogene **10**: 415-422.

Werner, H., G. G. Re, I. A. Drummond, V. P. Sukhatme, F. J. Rauscher, D. A. Sens, A. J. Garvin, D. Leroith and C. T. Roberts (1993). "Increased expression of the Insulin-Like growth Factor-I receptor gene, IGF1R, in wilms tumor is correlated with modulation of IGF1R promoter activity by the WT1 wilms tumor gene product." Proc Natl Acad Sci USA **90**(12): 5828-5832.

Werner, H., Z. Shen-Orr, F. J. Rauscher, J. F. Morris, C. T. Roberts and D. LeRoith (1995). "Inhibition of cellular proliferation by the Wilms' tumour suppressor WT1 is associated with suppression of insulin-like growth factor I receptor gene expression." Mol. Cell. Biol. **15**: 3516-3522.

Willetts, I. E. (2003). "Jessop and the Wilms' tumor." J Pediatr Surg **38**(10): 1496-8.

Yang, Y. and C. E. Walsh (2005). "Spliceosome-mediated RNA trans-splicing." Mol Ther **12**(6): 1006-12.

Zang, W. Q. and P. J. Romaniuk (1995). "Characterization of the 5 S RNA binding activity of Xenopus zinc finger protein p43." J Mol Biol **245**(5): 549-558.

Zang, W. Q., N. Veldhoen and P. J. Romaniuk (1995). "Effects of zinc finger mutations on the nucleic acid binding activities of Xenopus transcription factor IIIA." Biochemistry **34**(47): 15545-15552.

Zang, W. Q., N. Veldhoen and P. J. Romaniuk (1995). "Effects of zinc finger mutations on the nucleic acid binding activities of Xenopus transcription factor IIIA." Biochemistry **34**(47): 15545-52.

Zhai, G., M. Iskandar, K. Barilla and P. J. Romaniuk (2001). "Characterization of RNA aptamer binding by the Wilms' tumor suppressor protein WT1." Biochemistry **40**(7): 2032-40.